

Article

Solving Renewables-Integrated Economic Load Dispatch Problem by Variant of Metaheuristic Bat-Inspired Algorithm

Faisal Tariq ¹, Salem Alelyani ^{2,3}, Ghulam Abbas ^{1,*} , Ayman Qahmash ^{2,3} 
and Mohammad Rashid Hussain ^{2,3} 

¹ Department of Electrical Engineering, The University of Lahore, Lahore 54000, Pakistan; faisaltariq08170@gmail.com

² Center for Artificial Intelligence (CAI), King Khalid University, Abha 61421, Saudi Arabia; s.alelyani@kku.edu.sa (S.A.); a.qahmash@kku.edu.sa (A.Q.); humohammad@kku.edu.sa (M.R.H.)

³ College of Computer Science, King Khalid University, Abha 61421, Saudi Arabia

* Correspondence: ghulam.abbas@ee.uol.edu.pk or engrgabbas@gmail.com

Received: 27 September 2020; Accepted: 23 November 2020; Published: 26 November 2020



Abstract: One of the most important concerns in the planning and operation of an electric power generation system is the effective scheduling of all power generation facilities to meet growing power demand. Economic load dispatch (ELD) is a phenomenon where an optimal combination of power generating units is selected in such a way as to minimize the total fuel cost while satisfying the load demand, subject to operational constraints. Different numerical and metaheuristic optimization techniques have gained prominent importance and are widely used to solve the nonlinear problem. Although metaheuristic techniques have a good convergence rate than numerical techniques, however, their implementation seems difficult in the presence of nonlinear and dynamic parameters. This work is devoted to solving the ELD problem with the integration of variable energy resources using a modified directional bat algorithm (dBA). Then the proposed technique is validated via different realistic test cases consisting of thermal and renewable energy sources (RESs). From simulation results, it is observed that dBA reduces the operational cost with less computational time and has better convergence characteristics than that of standard BA and other popular techniques like particle swarm optimization (PSO) and genetic algorithm (GA).

Keywords: renewables incorporated ELD problem; directional bat algorithm (dBA); operational cost; convergence characteristics

1. Introduction

In a power system's operation and control, the cost of electric power generation is a major concern due to increased demand in residential and commercial sectors. Due to interconnection among distributed electrical networks, the reduction of electric energy charges is of utmost importance. Even a minor decrease in electric energy cost creates a huge impact on the economics of the overall power system. Economic load dispatch (ELD), a subset of the unit commitment problem, is considered an extremely significant problem that deals with the minimization of a power generation facilities' operational cost, where the primary job of power system engineers is to consider the economics of power systems. Moreover, the importance of this problem has greatly increased as it creates an impact on the environment. Economic dispatch also helps to minimize environmental pollutants to minimize fuel consumption. Furthermore, to improve the security of an electric system, there is also an utmost necessity to improve an ELD problem in terms of constraint to prevent any mishap like power system collapse.

The economics of any electric power system plays a significant role in encouraging researchers to find a technique that can reduce power generation cost up to a significant level. Traditionally, numerical techniques like gradient and Lambda iteration methods have been utilized to solve the ELD problem. However, due to the penetration of renewable energy resources, the optimization problem can add more complexity to nonlinear control variables. On the other hand, metaheuristic techniques are considered highly capable of solving high-dimensional ELD problems with less computational time. For example, in [1], a novel technique called the modified teaching-learning algorithm (MTLA) is presented. To overcome the convergence of the local optimum solution, a new stochastic self-adaptive mutation operator is introduced. Load forecast errors and contingencies of generating units are ignored in this research. In [2], modified particle swarm optimization (MPSO) is used to solve the ELD problem involving complex and non-continuous cost functions. This MPSO can deal with all types of constraints effectively. Furthermore, to speed-up the optimization process, a search space reduction strategy is proposed. In [3], an effort to find the optimum power combination of units at a minimum cost and under different power demands is performed using the augmented Lagrangian particle swarm optimization (ALPSO) technique. In [4], an improved PSO is used to solve the ELD problem, where a linearly decreasing inertia weight is combined with chaotic sequences to reduce the chances of premature convergence. However, this work does not consider strategies to reduce computational time for the high-dimensional ELD problem. In [5], authors proposed a mechanism to solve the ELD problem considering various practical constraints such as valve point loading (VPL) effects, ramp rate limits, prohibited operating zones (POZ), and multiple generator fuel options using the firefly algorithm and its variant, i.e., chaos mutation firefly algorithm (CMFA). The ability of the firefly algorithm is further enhanced by replacing the control parameters with fixed values. It is then achieved by self-adaption parameters, which affect solution quality, convergence speed, and reliability.

Similarly, in [6], a cuckoo search algorithm (CSA) is proposed for solving the nonconvex ELD problem by considering its various practical constraints. In [7], an enhanced bee swarm optimization method is utilized to solve a dynamic ELD problem, while maintaining a balance between exploration and exploitation. In [8], self-adaptive differential evolution and real coded genetic algorithm (GA) are proposed to solve the ELD problem. In [9], the dispatching of power is optimized using the firefly algorithm while avoiding the subjective penalty factors. In [10], a modified cuckoo search algorithm is proposed to solve the ELD problem considering VPL effects, POZ, losses, and ramp rate limits. This modification consists of self-adaptive step size and some neighbor study strategies to improve the performance of the standard cuckoo algorithm. With a high-dimensional test system, the efficiency of the proposed algorithm is tested. In [11], a modified version of PSO is presented for the ELD problem by considering different constraints. This makes the algorithm capable of search around feasible solution areas. In [12], more practical generator constraints like ramp rate limits and POZ are considered for the ELD problem. In [13], a quantum-inspired PSO is proposed to solve the ELD problem. By introducing quantum computing theory in the basic PSO, the searchability and convergence speed increases. In [14], an artificial immune system, evolutionary programming, and PSO are used for solving the ELD problem. In [15], novel PSO is applied to the ELD problem by considering the generator constraints. In the standard PSO, some mutation operators are introduced to improve its exploration capabilities. Mutation operators take charge as soon as the PSO velocity closes to zero or if it breaks lower and upper boundaries. PSO with mutation operators claims to outperform PSO easily. In [16], a detailed survey of PSO and its certain modifications is explained, while [17] deals with the hybridization of PSO with other algorithms to solve the ELD problem. In [18], ELD and combined economic and emission dispatch (CEED) problem is solved using an interior search algorithm (ISA). All the above-mentioned references are, however, used to solve all-thermal ELD problems that do not involve renewables.

However, a bat algorithm has also been found to solve all-thermal ELD problems successfully. In [19], the ELD problem is solved using a bat algorithm. The bat algorithm has proven to be better than PSO and the intelligent water drop (IWD) technique. The problem, however, does not include multiple

fuels and spinning reserve cases. In [20], two different cost functions are considered, i.e., smooth and non-smooth. A bio-inspired bat optimization problem (BOA) is used for the optimum setting of control variables. In [21], the ELD problem with a quadratic fuel function is solved using BA. It was proved that BA is capable of solving complex constraints problems with ease as it is easy to operate. In addition, the minimization of emission released was also completed. In [22], a BAT algorithm is utilized to solve the ELD problem. A mathematical model is presented for the ELD problem. In [23], some previous algorithms like GA, PSO, and BA are reviewed. The original BA is modified to enhance its capabilities. In [24], a multi-objective self-adaptive BA is introduced to solve a practical environmental and emission dispatch problem considering valve point effects, transmission losses, and ramp rate limits. BA is utilized to achieve Pareto optimal solutions. Novel self-adaptive learning is added to improve the diversity of the population. In [25], a chaotic bat algorithm (CBA), a variant of the bat algorithm, is used to solve the ELD problem. This variant is obtained by incorporating chaotic sequences in the original bat algorithm to improve its performance. This less tuning algorithm claimed to perform better than many algorithms. In [26], an enhanced BA is utilized to solve the ELD problem by considering different generator constraints. In [27], many of the variants of BA are reviewed and some new variants are introduced for enhancing the exploration and exploitation capability of this algorithm. In [28], the novel bat algorithm (NBA) is utilized to solve the ELD problem. In this variant of the bat algorithm, the doppler effect is introduced. Results claimed that NBA has much better efficiency and robustness than BA and PSO.

At present, renewables-incorporated ELD problems are gaining much more attention to cope with the challenge of an energy shortage and the environment and are being solved using metaheuristic techniques. In [29], a hybrid metaheuristic algorithm RCBA is presented to solve the ELD problem by incorporating thermal generators and renewables like wind power. This algorithm combines a chaotic map and random black hole model to avoid premature convergence and move towards the global area. In [30], the reliability of generators and uncertainty of wind power generation is dealt with. For considering extreme conditions with probability, forecasting error relating to wind power generation is modeled as a discretized beta probability distribution function (PDF). In [31], a solution of optimum power dispatch in an interconnected microgrid is presented. A probabilistic model is used for a balanced sharing of power at a minimum operating cost. PSO and imperialist competitive algorithm (ICA) are used for the optimization of the objective function. Results deduced claimed that optimal sharing between the main grid and microgrid decreases the distribution networks' cost. In [32], combined emission economic dispatch (CEED) is applied to a system consisting of thermal units and photovoltaic (PV) plants. The model considered is a mixed-integer optimization problem (MIOP) solved using PSO. In [33], ELD is solved using a dynamic adaptive bacterial foraging algorithm (BFA) with wind power incorporated. It was shown that this variant of BFA mitigates some drawbacks in the original BFA, such as poor convergence characteristics for high dimensional complex problems. In [34], a dynamic economic dispatch (DED) for the integration of large-scale renewable energy sources (RESs) with the ELD problem is reduced into dual stages using Lagrange relaxation where the multiplier is updated based on the quasi-Newton method. In [35], ELD considering wind power with forecast error is analyzed. As the wind uncertainty has a huge impact on power dispatch and a risk to the power grid, these forecast errors need to be minimized. In [36], the economic environmental dispatch problem is applied to a hybrid power system consisting of solar and wind energies. The strength Pareto evolutionary algorithm (SPEA) method is employed to solve this problem. In [37], the ELD problem considering RESs is solved using GA. It is shown that the inclusion of RESs impacts the economics of the system. However, this technique is not applied to the high-dimensional test case. In [38], the effect of substantial wind-based capacity on the economic load dispatch problem is considered. In [39], the ELD problem is considered with RESs. To deal with the uncertainty of wind and solar, their stochastic nature is modeled by Weibull and Beta distributions. An improved Fireworks algorithm is used to solve this highly-constrained problem. In [40], Lagrangian relaxation with the incremental proximal method is used to solve the ELD problem. In [41], combined emission economic dispatch

(CEED) is solved using the lighting flash algorithm by considering different cases with wind power penetration, multiple fuel options, and generator constraints. In [42], a cost-effective hybrid microgrid system is designed with renewable sources like wind, hydrogen-based storage systems, and fuel cells. This optimal power problem is solved using PSO and is further compared with GA. In [43], the ELD problem by a microgrid containing solar and wind farms is solved using the reduced gradient method. It is shown that solar energy should be incorporated with renewable energy credits. In [44], a control system is presented that is capable of maintaining constant voltage magnitude at the wind farm terminal. The ELD problem is applied to a system containing thermal and wind power units. In [45], the ELD problem is solved using the BAT algorithm by including wind power. In the overall objective function, the stochastic nature of wind power is taken into account. Furthermore, due to the forecasting errors, imbalance charges (overestimation, underestimation) are also considered.

Unlike other methods, the directional bat algorithm (dBA) evolved as a promising variant of BA is limitedly used to solve renewables-incorporated ELD problems that have recently received considerable scholarly attention. The dBA introduces the directional echolocation to the structure of BA, which may get trapped locally for the complex and constrained dispatch problems, so as to enhance exploitation and exploration characteristics. To validate the superiority of dBA, in this paper, the ELD problem with and without renewables considering different test cases is solved using BA and dBA. With the help of compelling results, it was proved that dBA converges faster with minimized fitness value, thus justifying the claim that it is more effective than BA and other well-known GA and PSO techniques.

The paper commences with the formulation of an ELD problem considering combined thermal and RESs in Section 2. Steps involved in the standard BA with advantages, disadvantages, and a few variants are highlighted in Section 3. Section 3 also introduces dBA and discusses the steps involved in implementing this technique. Section 4 shows the simulation results of the test cases with specific characteristics of particular cases. Finally, the findings of the paper are pointed out in Section 5.

2. Problem Formulation

The objective of this research is to minimize the operating cost of a thermal unit system by integrating solar PV and wind energy units, subject to power demand and dispatch limitations.

2.1. Thermal Energy

The cost function of a thermal power plant without and with the valve point effect (VPL) is a second-order polynomial function:

$$F_i(P_i) = \begin{cases} a_i P_i^2 + b_i P_i + c_i & \text{without VPL} \\ a_i P_i^2 + b_i P_i + c_i + |e_i \times \sin(f_i \times (P_i^{\min} - P_i))| & \text{with VPL} \end{cases} \quad (1)$$

where a , b , c , e , and f are fuel cost coefficients of power generation unit i whereas the total cost of j thermal units is expressed by $\sum_{i=1}^j F_i(P_i)$.

2.2. Wind Energy

The power generated by wind turbines can be written as:

$$P_w = \frac{1}{2}(\rho A u^3) \quad (2)$$

where ρ is the air density, u^3 is wind speed, and A is the windswept area, respectively. The cost function of wind generation is subject to the investment cost of the equipment and the operation and

maintenance (O&M) cost of generated energy. However, the capital cost of land, assuming it is a community-based microgrid where the land is owned by the community [43] is given as:

$$F(P_w) = aI^P P_w + G^E P_w \quad (3)$$

where a can be expressed as:

$$a = \frac{r}{[1 - (1 + r)^{-N}]} \quad (4)$$

where P_w is the wind generation in (kW), a is an annuitization coefficient (dimensionless), r is the interest rate (taken as 0.09 for base case), N is the investment lifetime ($N = 20$ years), I^P is the investment cost per unit installed power (\$/kW), and G^E is the O&M cost per unit of generated energy (\$/kW), respectively. In this system, it is assumed that I^P and G^E are approximately equal to \$1400 and 1.6 cents per kW, respectively.

2.3. Solar PV Energy

The maximum power provided by a solar panel is given by [43]:

$$E_t = 3.24M_{PV}(1 - 0.0041 \times (T_t - 8) \times S_t) \quad (5)$$

where E_t is the output power, M_{PV} is the capacity of each PV panel, T_t is the temperature, and S_t is the radiation data at time i , respectively. The cost function of solar generation in [43] involves the investment cost of the equipment and the O&M cost of the generated energy. However, without the capital cost of land, it can be expressed as:

$$F(P_s) = aI^P P_s + G^E P_s \quad (6)$$

where a is written as:

$$a = \frac{r}{[1 + (1 + r)^{-N}]} \quad (7)$$

where P_s is the solar generation (kW), a is an annuitization coefficient (dimensionless), r is the interest rate (taken as 0.09 for base case), N is the investment lifetime (taken as $N = 20$ years), I^P is the investment costs per unit installed power (\$/kW), and G^E is the O&M cost per unit generated energy (\$/kW), respectively). In this system, it is assumed that the investment costs per unit installed power (I^P) and O&M cost per unit generated energy (G^E) are approximately equal to \$5000 and 1.6 cents per kW, respectively.

In the case of RESs, the generating cost parameter is not taken into account. The RESs that are considered in this research are wind energy and solar PV energy, whose forecasting is taken from [43] and is shown in Figure 1. A comprehensive review of the forecasting approaches for wind and solar power generation can be found in [46].

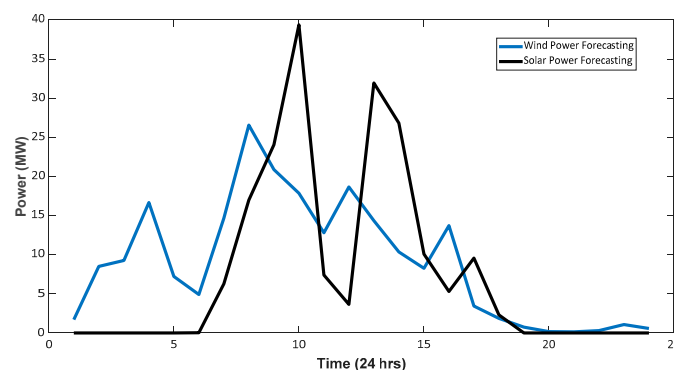


Figure 1. Wind and solar power forecasting.

2.4. Overall Cost Function Incorporating Renewables

Adding all the cost functions described in (1), (3), and (6) gives the overall cost function as:

$$F_T = F_i(P_i) + F(P_w) + F(P_s) \quad (8)$$

The following constraints (equalities and inequalities) have been considered while minimizing the overall cost function.

Power Balance Equation: Neglecting the transmission losses, the total generated power of all the units (thermals and renewables) $\sum_{i=1}^n (P_i)$ should be equal to the total system demand P_{Load} , i.e.,

$$\sum_{i=1}^n (P_i) = P_{Load}$$

Generator Capacity Limits: The power delivered by each generating unit should remain within its minimum and maximum limits.

$$P_{i,\min} \leq P_i \leq P_{i,\max}$$

where $P_{i,\min}$ and $P_{i,\max}$ signify the i th generating unit's minimum and maximum output power, respectively.

3. A Variant of BA for the ELD Problem

3.1. Overview of BA

This algorithm is inspired by microbats. The rules followed by this algorithm emerge from the certain behavior of bats, which are discussed as follows [47]:

1. Bats use echolocation to sense distance and to know the difference between food and prey. In our case, the fitness function is food and bats, which are the possible solutions;
2. The bats fly randomly with some predefined velocity v_i at a position x_i with a predefined frequency f_i . They can adjust their frequency of pulse emitted;
3. They can vary the rate of pulses by looking at the target proximity;
4. Loudness can be varied from a large positive value to a small value.

Figure 2 shows the flowchart involved in the process. The algorithm progresses by taking the following steps:

1. Firstly, we initialize the algorithm with maximum iterations, bat population, loudness constant α , pulse rate constants γ , initial values of loudness, and pulse rates;
2. Give a random position to all bats in the solution space within the lower and upper boundary;
3. Find the best bat position x^* and its fitness;
4. Start the process in which the position is updated one by one by:

$$\begin{aligned} f_i &= f_{\min} + (f_{\max} - f_{\min})\beta \\ v_i &= v_i^{t-1} + (x_i^{t-1} - x^*)f_i \\ x_i^t &= x_i^{t-1} + v_i^t \end{aligned} \quad (9)$$

where v_i^t is the velocity of bat i at a certain position x_i^t at iteration t . There is the global best position x^* among all the bats. Minimum and maximum frequency is selected depending on the application. The value β will be between 0 and 1.

5. Now a random number is generated (between 0 and 1) and is compared with pulse rate. Based on pulse rate, local search is done around the best solution by:

$$x_{new} = x_{old} + \varepsilon A^t \quad (10)$$

6. An existing random solution k is selected with $k \neq i$ and is compared with the new solution. If it is better, then update the new solution by:

$$x_{new} = x_k + \varepsilon A^t \quad (11)$$

7. The new solution from the previous step will be compared with the existing positions of the current bat. Furthermore, a random number will again be generated and compared with loudness A_i^t of that bat. If the new solution of the previous step is better than the global best solution, and the random number is less than loudness, then a new solution will be accepted, and the loudness and pulse rate of that bat will be updated based on the following expressions:

$$\begin{aligned} A_i^{t+1} &= \alpha A_i^t \\ r_i^{t+1} &= r_i^0 [1 - e^{(-\gamma t)}] \end{aligned} \quad (12)$$

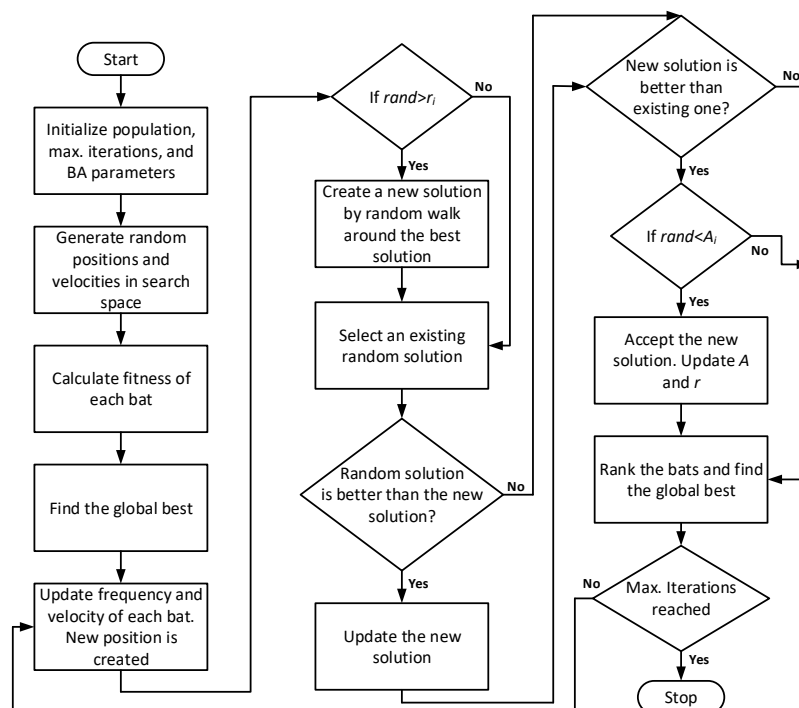


Figure 2. Flow chart of the bat algorithm (BA).

Loudness and pulse rates play a vital role in finding the best result in terms of control exploration and exploitation. The value of loudness will decrease from a positive value to a certain minimum value, while the pulse rate will increase from a small value to a large value as the bat finds its prey. α and γ are the constants of loudness and pulse rate, and the value of α will be any value between 0 and 1 and γ is greater than 0. Optimum values of α and γ have been selected as 0.9 and 0.98, respectively [47].

Although the bat algorithm comes with the advantages of having a highly efficient, reliable, easy structure and can be programmed from any programming language easily, it suffers from limitations of premature convergence, which increases with complexity and bat moves by the information from the best bat (best bat could be local optimum). This requires a modification in the

structure of the BA to handle the nonconvex ELD problem. Much research has been done to improve the exploration and exploitation capabilities of the BA. There are many variants of the BA [27]. Some of the variants, such as the novel BA [28], enhanced BA [26], chaotic BA [25], and modified BA [23] have already been applied to solve the ELD problem. In this paper, we are going to apply a dBA to tackle the renewables-incorporated ELD problem.

3.2. dBA

dBA plays a dual role at different stages of the algorithm. In the beginning, it helps to explore more search space and as the process moves, the bats move around the leader, which improves the exploitation ability. It has a strong exploitation process that increases the convergence speed without being trapped in local optima. By adding a scale factor in the local search step, bats are allowed to move randomly with large steps. This results in enhancing the exploration capability of the algorithm. A decrease in the scale factor as the iteration proceeds improves the exploitation capability [48,49].

The procedure followed by dBA is very similar to the original BA; however, some modifications are made to improve its diversification and intensification [48,49]. Figure 3 shows the flow chart involved in the dBA process.

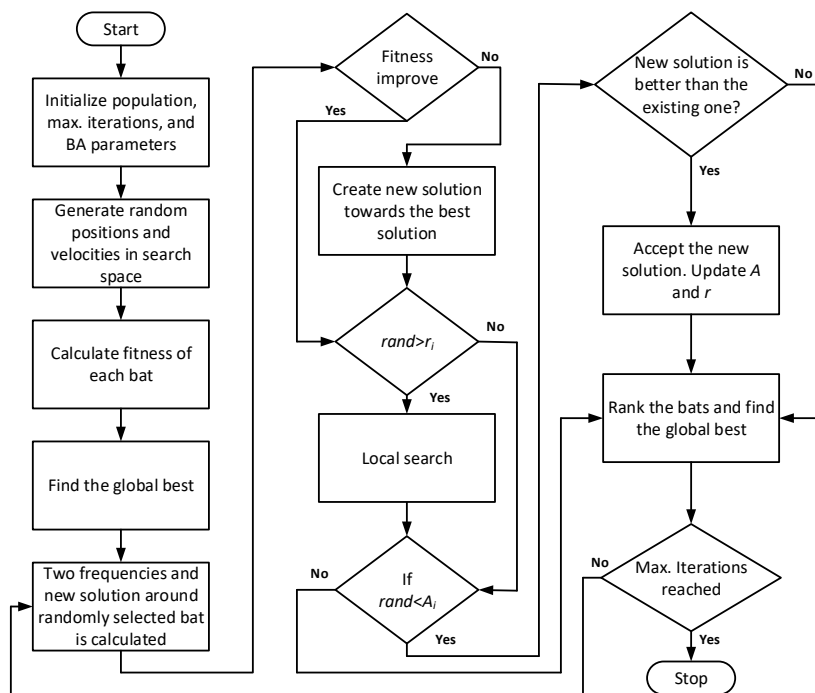


Figure 3. Flow chart of the directional bat algorithm (dBA).

1. Firstly, bats are initialized by giving random positions within the upper and lower boundaries of each bat;
2. The standard BA has two navigation modes: First, towards the best solution and second, to exploit the best solution. In directional echolocation, bats move by analyzing their echoes. In addition, a bat takes help from other bats for better decisions. One of the bat pulses is toward the leader and another one toward a randomly selected bat. If the food exists around that random bat, the bat moves toward it otherwise, it moves toward the leader (best bat). Equations (13) and (14) depict this movement as follows:

$$x_i^{t+1} = x_i^t + (x^* - x_i^t)f_1 + (x_k^t - x_i^t)f_2 \quad (13)$$

If the food does not exist around the random bat, then a bat will move towards the leader:

$$x_i^{t+1} = x_i^t + (x^* - x_i^t)f_1 \quad (14)$$

where x_k^t shows the position of randomly selected bat k where $k \neq i$ and x^* shows the position of the global best. In the above equations, f_1 and f_2 are the frequencies of two pulses which are assigned as:

$$\begin{aligned} f_1 &= f_{\min} + (f_{\max} - f_{\min})rand1 \\ f_2 &= f_{\min} + (f_{\max} - f_{\min})rand2 \end{aligned} \quad (15)$$

where $rand1$ and $rand2$ are random numbers between 0 and 1;

3. In the next step, the local search step is done similar to BA. However, the equation is modified by including a scale factor w_i^t as follows:

$$x_i^{t+1} = x_i^t + \langle A^t \rangle \varepsilon w_i^t \quad (16)$$

where $\langle A^t \rangle$ is the average loudness and ε has a random value between -1 and 1 . The value of w_i^t starts from a large value and then reduces to 1% of a quarter of its length as follows:

$$w_i^t = \left(\frac{w_{i0} - w_{i\alpha}}{1 - t_{\max}} \right) (t - t_{\max}) + w_{i\alpha} \quad (17)$$

where w_{i0} and $w_{i\alpha}$ show the initial and final values, respectively, and t and t_{\max} show the current and maximum iteration, respectively. The value of w_{i0} and $w_{i\alpha}$ can be set as:

$$\begin{aligned} w_{i0} &= (U_i - L_i) / 4 \\ w_{i\alpha} &= w_{i0} / 100 \end{aligned} \quad (18)$$

Here U_i and L_i show the upper and lower bounds, respectively;

4. In the next step, which is similar to the standard BA, a random number is compared with loudness, but unlike the standard BA, a new solution is compared with the existing solution of that bat (not the global best). This step helps to improve the diversity of the algorithm. If these two conditions are true, then only new solutions are accepted. The pulse rate has an important role as it decides a balance between exploration and exploitation. Moreover, the loudness and pulse rate are updated as follows:

$$\begin{aligned} A^t &= \left(\frac{A_0 - A_\infty}{1 - t_{\max}} \right) (t - t_{\max}) + A_\infty \\ r^t &= \left(\frac{r_0 - r_\infty}{1 - t_{\max}} \right) (t - t_{\max}) + r_\infty \end{aligned} \quad (19)$$

where A and r show the loudness and pulse rate, respectively. For the best results, the optimum values recommended in the literature are 0.1 and 0.7 for pulse rate, and 0.9 and 0.6 for loudness;

5. In the last step, the new solution is compared with the global solution. If it has better fitness, then the global solution is updated [48,49].

4. Simulation Results and Discussion

To validate the successful application of dBA to the ELD problem and to show its superiority over GA, PSO, and BA, two test systems, namely an IEEE 57-bus system with 7 thermal units driving from fossil fuels and a high dimensional 15-unit system, with and without renewables, are considered. A MATLAB environment was used to solve the test systems. Unless otherwise specified, for all the simulation results, the population and iteration were selected at 100 and 1000, respectively for all considered optimization algorithms. For BA and dBA algorithms, the values of f_{\min} and f_{\max} were set to 0 and 2, respectively, whereas $r_0 = 0.1$, $r_{\max} = 0.7$, $A_0 = 0.9$, and $A_{\max} = 0.6$. For PSO, inertial, personal, and global coefficients were set to 0.9, 2, and 2, respectively. For GA, the selection strategy

was stochastic uniform, the mutation function was adaptive feasible, and the crossover probability was set to 0.8. The selection of the parameters is made on the basis of the experiments to ensure a better solution.

4.1. Case 1: The IEEE 57 Bus System with Seven Thermal Units

4.1.1. Data

An IEEE 57 bus system, which consists of 7 thermal units running from fossil fuels, was considered. The cost coefficients with minimum and maximum power generation limits are shown in Table 1 [50]. In Table 2, a 24 h load forecasting was selected as a load demand which was to be met. It can be seen that the maximum power demand at 1600 h is 1800 MW. In this case, $F_{thermal} = \sum_{i=1}^7 F_i(P_i)$.

Table 1. Cost coefficients of seven thermal units with lower and upper power limits.

Generator	a (\$/MW ²)	b (\$/MW)	c (\$)	P_{min} (MW)	P_{max} (MW)
1	0.007	7	400	100	575
2	0.0095	10	200	50	100
3	0.009	8.5	220	50	140
4	0.009	11	200	50	100
5	0.008	10.5	240	100	550
6	0.0075	12	200	50	100
7	0.0068	10	180	100	410

Table 2. Demand forecasting over 24 h.

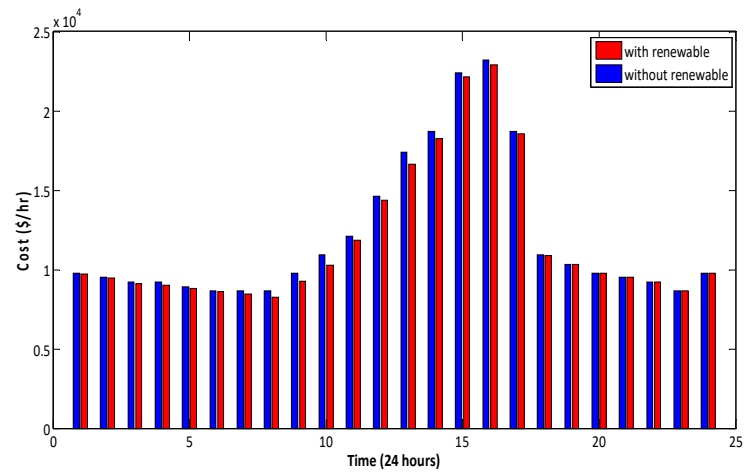
Time (h)	1	2	3	4	5	6	7	8	9	10	11	12
Demand (MW)	800	780	750	750	720	700	700	700	800	900	1000	1200
Time (h)	13	14	15	16	17	18	19	20	21	22	23	24
Demand (MW)	1400	1500	1750	1800	1500	900	850	800	780	750	700	800

The data used for RESs are mentioned where the renewables-incorporated ELD problem is discussed in the following sections/subsections.

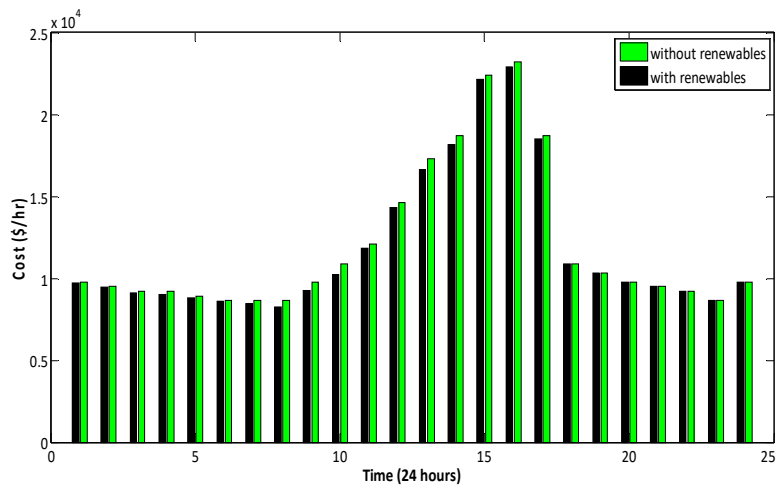
4.1.2. Cost Offered by BA and dBA

Table 3 shows the simulation results of BA and dBA in terms of operating costs for a 24 h period. It can be seen that dBA comparatively gives a lower operating cost, i.e., 288,526 \$/day than that of BA which gives 288,673 \$/day. Even for the load demand for each hour, dBA ensured less cost when compared to BA. This ensures that dBA displays a better chance of finding the solution closer to the global optimum with regard to the conventional BA. In the second scenario, a seven-unit thermal system was added with one wind and one solar PV farm. Both BA and dBA were applied to ELD incorporating renewables. Table 4 shows the result of BA and dBA over a 24 h time period. It is clear from the results that dBA gives better fitness results when compared to the BA. The dBA is found more successful in reducing the total cost per day as compared to dBA with or without renewables.

From Figure 4, it can be seen that the operating cost of the system decreases with the incorporation of solar and wind farms in the system.



(a)



(b)

Figure 4. Cost offered by (a) BA and (b) dBA without and with considering renewables.

Table 3. BA and dBA on a seven-thermal unit system without renewables.

<i>t</i> (h)	BA								dBA									
	<i>P</i> ₁ (MW)	<i>P</i> ₂ (MW)	<i>P</i> ₃ (MW)	<i>P</i> ₄ (MW)	<i>P</i> ₅ (MW)	<i>P</i> ₆ (MW)	<i>P</i> ₇ (MW)	Cost (\$/h)	<i>P</i> ₁ (MW)	<i>P</i> ₂ (MW)	<i>P</i> ₃ (MW)	<i>P</i> ₄ (MW)	<i>P</i> ₅ (MW)	<i>P</i> ₆ (MW)	<i>P</i> ₇ (MW)	Cost (\$/h)		
1	310.0691	50.4229	139.3672	50	100.1412	50	100	9762.3	298.4298	61.5703	140	50	100	50	100	9759.8		
2	290.9093	50	139.0909	50	100	50	100	9538.2	286.5761	53.9338	139.4902	50	100	50	100	9537.9		
3	272.9545	50	127.0456	50	100	50	100	9210.4	272.0187	50.0043	127.9772	50	100	50	100	9210.3		
4	274.7427	50	125.2577	50	100	50	100	9210.5	271.5529	50	128.4458	50.0014	100	50	100.0001	9210.3		
5	259.4567	51.3485	108.9565	50.2387	100	50	100	8891	255.0398	50	114.96	50	100.0003	50	100	8889.7		
6	245.5637	50	104.4364	50	100	50	100	8679.9	243.9639	50.0033	106.0329	50	100	50	100	8679.9		
7	246.6246	50	103.3755	50	100	50	100	8680	243.7256	50	106.2745	50.0001	100	50	100	8679.9		
8	238.2873	50	111.7129	50	100	50	100	8680.4	243.5853	50	106.4148	50	100	50	100	8679.9		
9	296.9272	63.8645	139.2085	50	100	50	100	9760	298.3961	61.604	140	50	100	50	100	9759.8		
10	358.2764	99.7169	139.9486	50.5802	100.3323	50.5205	100.6255	10,918	338.785	92.757	140	50.1718	100	50	128.2864	10,909		
11	375.1164	98.3909	139.0237	62.0253	100	50	175.4441	12,112	371.9944	100	140	67.441	107.4991	50	163.0657	12,108		
12	412.0067	99.8622	139.8622	99.8622	160.4408	78.8337	209.1325	14,631	426.0054	99.9996	140	100	151.3067	64.2512	218.4388	14,626		
13	574.5894	99.4245	139.5894	96.7237	163.8266	99.4364	226.4103	17,386	481.1635	99.9997	140	100	203.4979	100	275.3393	17,292		
14	517.2808	99.9756	139.9756	99.9756	215.7508	99.9756	327.0668	18,695	516.7083	99.9966	139.9939	99.9827	231.9789	100	311.3399	18,691		
15	574.9994	99.9994	139.9994	99.9994	325.004	99.9994	409.9994	22,406	575	100	140	100	325	100	410	22,406		
16	574.9815	99.9815	139.9815	99.9815	375.1116	99.9815	409.9815	23,212	575	100	140	100	375	100	410	23,211		
17	509.9228	99.8615	139.8615	99.8615	255.8211	99.8615	294.8103	18,698	516.0237	100	139.9982	100	233.6462	99.9773	310.3549	18,691		
18	360.6688	99.0931	139.9944	50.061	100.061	50.061	100.061	10,918	338.5833	92.8095	140	50.0021	100	50	128.6058	10,909		
19	323.4386	68.3125	139.1759	50	100	50	119.0736	10,330	320.393	78.0468	140	50	100	50	111.5603	10,328		
20	289.5354	68.0608	139.8835	50.6302	100.6302	50.6302	100.6302	9762.9	298.3036	61.6965	140	50.0001	100	50	100	9759.8		
21	291.5612	50	138.4389	50	100	50	100	9538.2	290	50	140	50	100	50	100	9538.1		
22	261.7829	50	138.2172	50	100	50	100	9212	271.6896	50.0002	128.3102	50	100	50.0004	100	9210.3		
23	243.2984	50	106.7019	50	100	50	100	8679.9	244.0813	50	105.9188	50	100	50	100	8679.9		
24	310.4408	50	139.5594	50	100	50	100	9762.2	298.0959	61.9043	140	50	100	50	100	9759.8		
	Total Cost (\$/day)								288,673	Total Cost (\$/day)								288,526

Table 4. BA and dBA on a seven-thermal unit system with renewables (wind and solar).

<i>t</i> (h)	BA										dBA													
	<i>P</i> ₁ (MW)	<i>P</i> ₂ (MW)	<i>P</i> ₃ (MW)	<i>P</i> ₄ (MW)	<i>P</i> ₅ (MW)	<i>P</i> ₆ (MW)	<i>P</i> ₇ (MW)	Wind (MW)	Solar (MW)	Cost (\$/h)	<i>P</i> ₁ (MW)	<i>P</i> ₂ (MW)	<i>P</i> ₃ (MW)	<i>P</i> ₄ (MW)	<i>P</i> ₅ (MW)	<i>P</i> ₆ (MW)	<i>P</i> ₇ (MW)	Wind (MW)	Solar (MW)	Cost (\$/h)				
1	308.4546	50	139.8458	50	100	50	100	1.7	0	9742.92	297.5162	60.7842	139.9997	50.0001	100	50	100	1.7	0	9740.8				
2	282.318552	4.223	136.7595	50	100	50	100	8.5	0	9444.65	283.6469	50.0558	137.7975	50	100	50	100	8.5	0	9444.6				
3	262.3932	50	128.3369	50	100	50	100	9.27	0	9110.95	266.8788	50	123.8513	50	100	50	100	9.27	0	9110.7				
4	258.6982	50	124.6419	50	100	50	100	16.66	0	9031.9	262.9667	50	120.3733	50	100	50	100.0001	16.7	0	9031.7				
5	243.8264	50	118.9539	50	100	50	100	7.22	0	8814.52	250.6062	50	112.1739	50	100	50	100	7.22	0	8813.7				
6	248.2989	50	96.7612	50	100	50	100	4.91	0.03	8629.47	241.1867	50	103.8734	50	100	50	100	4.91	0.03	8628.6				
7	240.6063	50	88.4639	50	100	50	100	14.66	6.27	8465.19	232.0606	50	97.0095	50	100	50	100	14.7	6.27	8464				
8	217.1576	50	89.3027	50	100	50	100	26.56	17	8234.75	219.1811	50	87.279	50	100	50.0001	100	26.6	17	8234.7				
9	265.3591	50	139.7113	50	100	50	100	20.88	24.1	9267.36	275.0707	50	129.997	50	100	50.0024	100	20.9	24.1	9266				
10	348.458650	8.649	139.997450	8.649	100.864950	8.649	100.864917	8.5	39.4	10,260.6	319.7501	76.1018	139.9973	50	100.001350	0.001	106.93	17.9	39.4	10,246				
11	374.550998	4.651	139.613167	5.442	101.6685	50	147.9493	12.8	7.41	11,864.4	365.1241	99.9767	140	63.0469	104.1673	50	157.4756	12.8	7.41	11,863				
12	451.210298	5.168	139.419798	5.708	100	50	239.982918	6.5	3.65	14,373.3	418.8554	100	140	99.0082	149.230159	5.93	211.0165	18.7	3.65	14,339				
13	468.176999	8.158	139.815899	8.158	190.391699	8.158	255.878914	3.5	31.9	16,662.8	467.1655	100	140	100	188.8588	100	257.6867	14.4	31.9	16,662				
14	574.983799	9.837	139.983799	9.837	216.070950	1.673	281.667610	3.5	26.8	18,249.8	504.4502	100	140	100	222.0573	100	296.3327	10.4	26.8	18,166				
15	574.981399	9.813	139.981399	9.813	306.773299	9.813	409.9813	8.26	10.1	22,121.6	575	100	140	100	306.66	100	410	8.26	10.1	22,121				
16	574.998199	9.981	139.998199	9.981	356.002399	9.981	409.998113	7.1	5.3	22,900.9	575	100	140	100	355.99	100	410	13.7	5.3	22,901				
17	574.033999	7.617	139.967199	9.671	204.820899	9.671	268.4729	3.44	9.57	18,548.5	511.3355	100	140	99.9984	229.8833	100	305.7731	3.44	9.57	18,506				
18	330.592797	9.07	134.696152	3.771	100	50	130.2475	1.87	2.31	10,865	338.3721	91.9396	140	50.0246	100	50	125.4839	1.87	2.31	10,860				
19	329.274	50.2884	139.987950	2.884	100.288450	2.884	128.8352	0.75	0	10,330.1	321.3166	77.8541	139.9876	50	100	50.0083	110.0839	0.75	0	10,319				
20	310.3985	50	139.4316	50	100	50	100	0.17	0	9760.36	309.83	50	140	50	100	50	100	0.17	0	9760.2				
21	284.235356	3.57	139.2578	50	100	50	100	0.15	0	9536.4	286.8948	52.9553	140	50	100	50	100	0.15	0	9536.3				
22	264.029	51.4983	134.1629	50	100	50	100	0.31	0	9207.99	272.0281	50	127.662	50	100	50	100	0.31	0	9207				
23	244.2126	50	104.7176	50	100	50	100	1.07	0	8668.77	243.2655	50	105.6646	50	100	50	100	1.07	0	8668.8				
24	302.386557	3.543	139.6794	50	100	50	100	0.58	0	9753.69	297.7595	61.6605	140	50.0002	100	50	100	0.58	0	9753.3				
Total Cost (\$/day)										283,846					Total Cost (\$/day)					283,642				

4.1.3. Characteristics Offered by BA and dBA

Figures 5–9 show the various characteristics of the BA and dBA against test case 1. Figures 5 and 6 show the position of bats for the BA and dBA, respectively. As shown, bats start from random locations (initial solutions) and converge to the best solution after 1000 iterations. However, in the case of dBA, the bats are much better optimized. Figure 7a shows that fitness offered by the BA decreases quickly, which increases the risk of trapping the optimal solution in the local optimum. However, fitness gradually decreases as the iterations progress in the case of dBA. It has a better chance of moving closer to the global optimum. Figure 7b shows the magnified view of the cost convergence curve. Figure 8 shows the pulse rate of the best bat which depicts the decrease of pulse rate as the bat finds its prey. Figure 9 shows the best bat's loudness, which depicts the increase of loudness as the bat finds its prey.

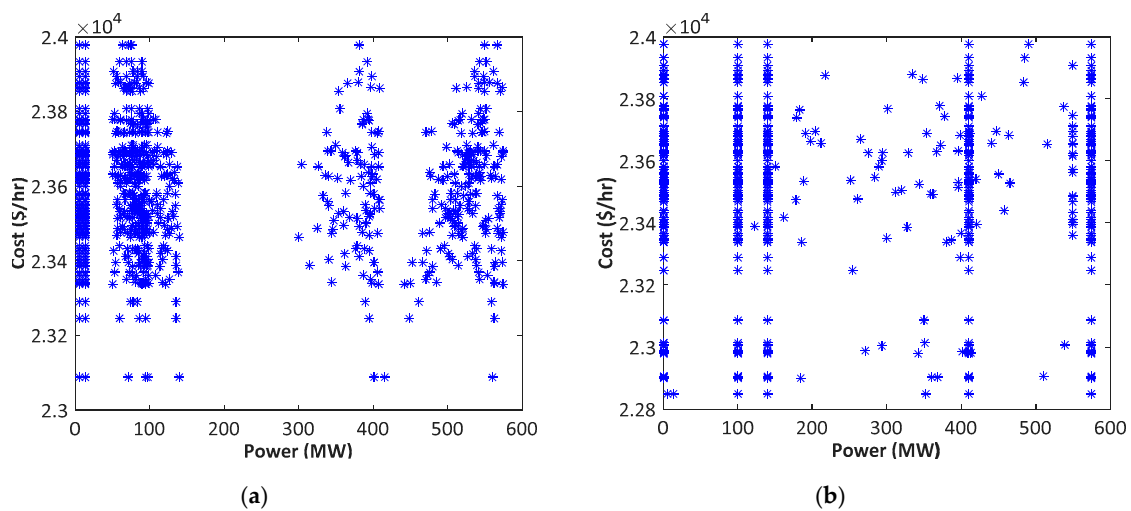


Figure 5. Bats positions in the BA (a) at the start and (b) after 1000 iterations (seven-unit system with renewables).

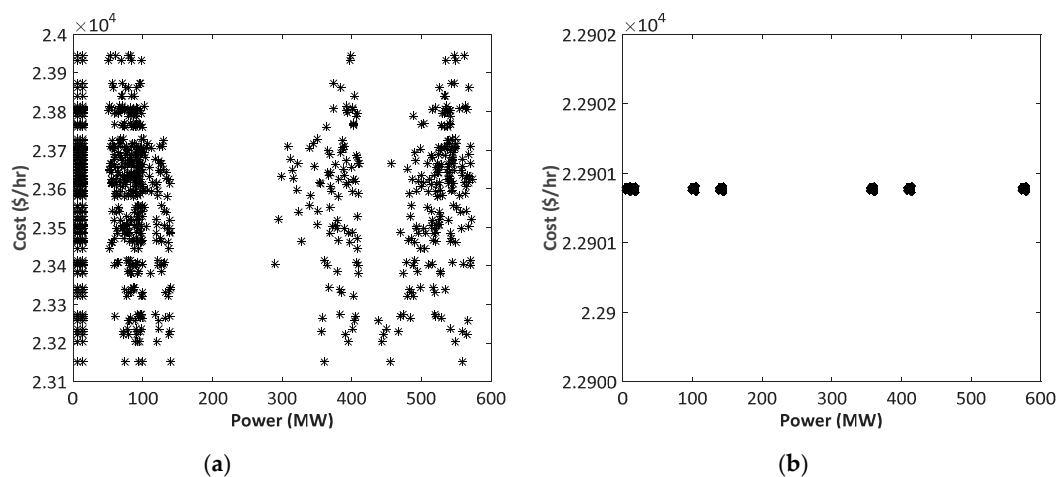
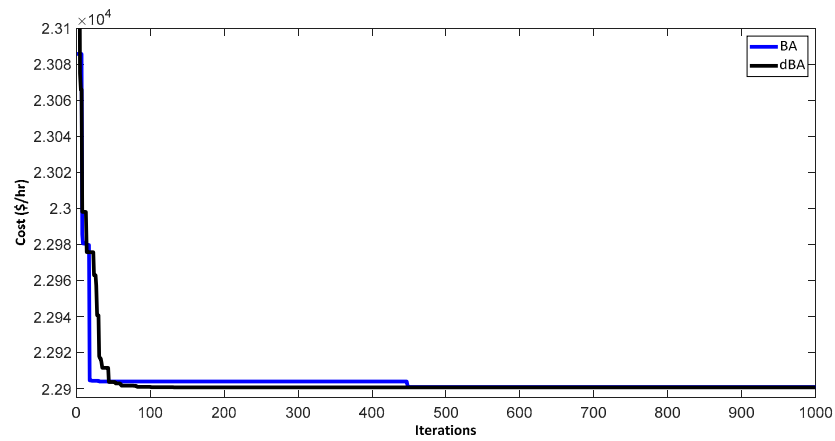
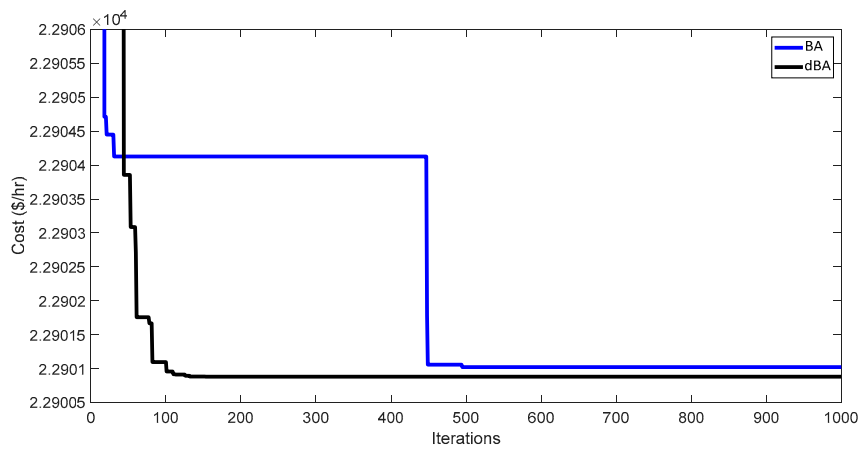


Figure 6. Bats positions in the dBA (a) before and (b) after 1000 iterations (seven-unit system with renewables).



(a)



(b)

Figure 7. Convergence curve: (a) The cost convergence curve by the BA and dBA (seven-unit system with renewables); (b) Magnitude view.

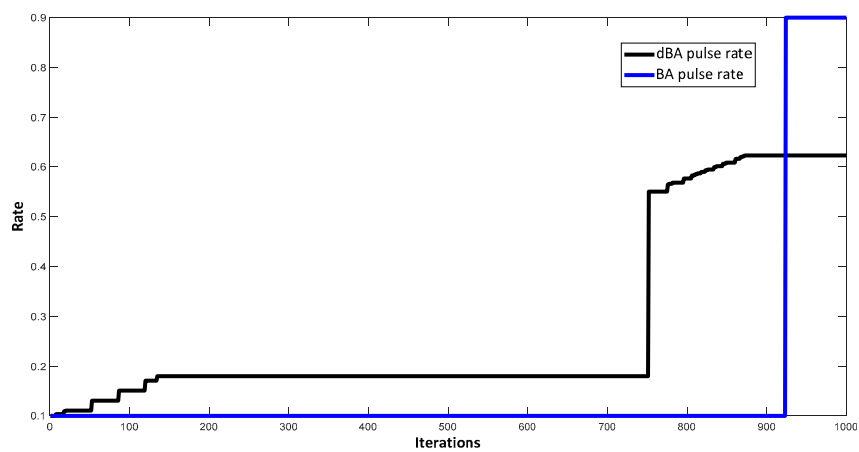


Figure 8. The pulse rate of the best bat of the BA and dBA.

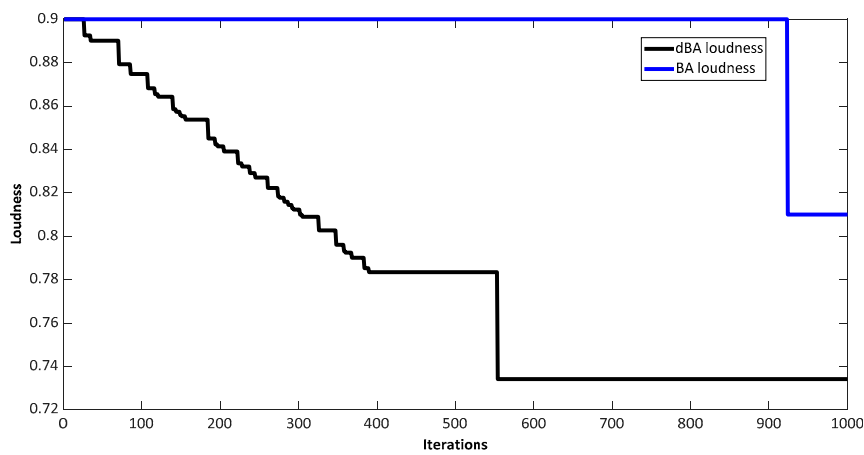


Figure 9. The loudness of the best bat of the BA and dBA.

4.1.4. Comparison of dBA, BA, PSO, and GA

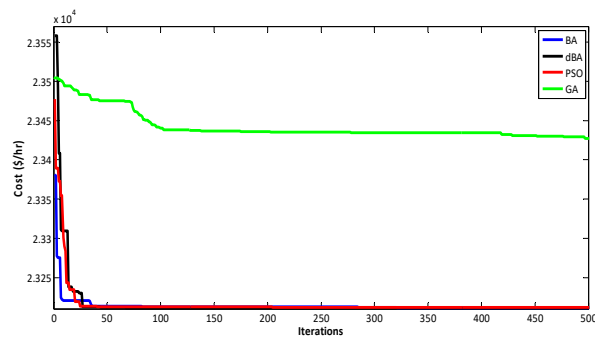
To further justify the effectiveness of the dBA over BA and other metaheuristic techniques like PSO and GA, a test case of 1800 MW was taken with 100 population and 1000 iterations. Tables 5 and 6 show the results regarding cost without and with renewables, respectively. It can be seen that the dBA is better when compared to BA, which in turn dominates PSO and GA. Figure 10 shows the convergence graph without renewables, whereas Figure 11 shows the convergence with renewables.

Table 5. Cost comparison for 1800 MW demand without renewables.

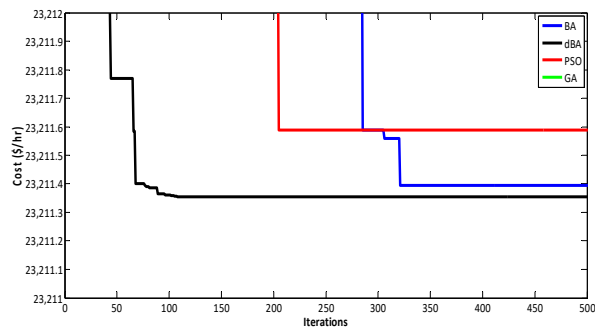
Algorithm	P_1 (MW)	P_2 (MW)	P_3 (MW)	P_4 (MW)	P_5 (MW)	P_6 (MW)	P_7 (MW)	Cost (\$/h)
GA	495.2	99.9987	140	99.9905	454.884	99.978	409.916	23,422.78
PSO	575	100	140	100	375.014	100	410	23,211.59
BA	575	99.998	140	99.998	375.012	99.998	409.998	23,211.39
dBA	575	100	140	100	375	100	410	23,211.36

Table 6. Cost comparison for 1800 MW demand with renewables.

Algorithm	P_1 (MW)	P_2 (MW)	P_3 (MW)	P_4 (MW)	P_5 (MW)	P_6 (MW)	P_7 (MW)	Wind (MW)	Solar (MW)	Cost (\$/h)
GA	486.477	99.95	139.988	99.8611	446.64	99.9438	408.14	13.7	5.3	23,124.8
PSO	575	100	140	100	356	100	410	13.71	5.3	22,901.1
BA	574.992	99.99	139.992	99.992	356.04	99.992	409.99	13.71	5.3	22,901.0
dBA	575	100	140	100	355.9	100	410	13.71	5.3	22,899.4

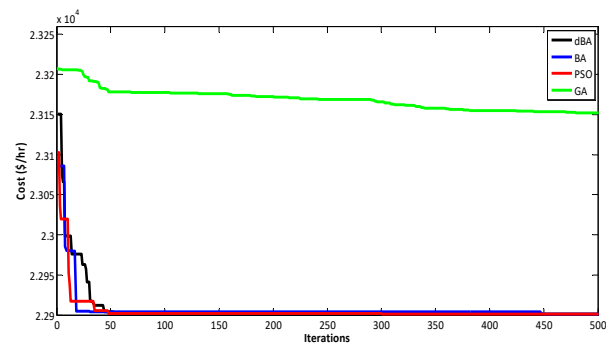


(a)

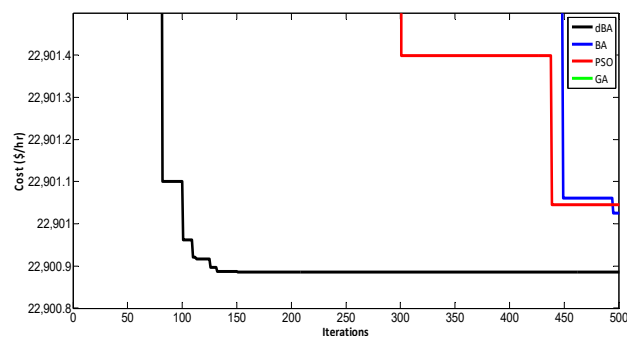


(b)

Figure 10. Convergence curve: (a) Convergence graphs without renewables; (b) Magnified view.



(a)



(b)

Figure 11. Convergence curve: (a) Convergence graphs with renewables; (b) Magnified view.

4.2. Case 2: A 15 Thermal Unit System

4.2.1. Data

The data for a 15-unit system is taken from [12], whereas the solar and wind forecasting data is taken from [43]. Table 7 shows the cost coefficients and the minimum and maximum power limits of all 15 thermal units. Table 8 shows the demand forecasting taken into consideration for this case.

Table 7. 15-unit system cost coefficients with lower and upper power limits.

Generator	a (\$/MW ²)	b (\$/MW)	c (\$)	P_{\min} (MW)	P_{\max} (MW)
1	0.000299	10.1	671	150	455
2	0.000183	10.2	574	150	455
3	0.001126	8.8	374	20	130
4	0.001126	8.8	374	20	130
5	0.000205	10.4	461	150	470
6	0.000301	10.1	630	135	460
7	0.000364	9.8	548	135	465
8	0.000338	11.2	227	60	300
9	0.000807	11.2	173	25	162
10	0.001203	10.7	175	25	160
11	0.003586	10.2	186	20	80
12	0.005513	9.9	230	20	80
13	0.000371	13.1	225	25	85
14	0.001929	12.1	309	15	55
15	0.004447	12.4	323	15	55

Table 8. Demand forecasting over 24 h.

Time (h)	1	2	3	4	5	6	7	8	9	10	11	12
Demand (MW)	1650	1680	1680	1700	1700	1700	2000	2000	2500	2500	2700	2800
Time (h)	13	14	15	16	17	18	19	20	21	22	23	24
Demand (MW)	2900	3000	3000	3000	3000	2800	2500	2000	1800	1750	1700	1700

4.2.2. Cost Offered by the BA and dBA

In the first scenario where renewables are not taken, both the BA and dBA are applied to a 15-thermal unit system for a 24 h period, and the result is shown in Tables 9 and 10, respectively. The bat population and iterations are taken as 100 and 1000, respectively. It can be seen that the dBA gives better fitness when compared to the BA. Similarly, in the second scenario where renewables are taken, both BA and dBA were applied to 15 thermal units with renewables (one solar and one wind farm) added for 24 h, and the results are shown in Tables 11 and 12, respectively. For this scenario, the dBA outperforms the BA in terms of (cost) fitness. The dBA offers not only a minimum cost per day but also a minimum hourly cost. The dBA is found to be more successful in optimizing the total operating cost per day than the BA with or without renewables.

From the above results, it can be seen that the incorporation of solar and wind farms into the 15-unit thermal system saves 4458 \$/day in the case of the BA and approximately 4215 \$/day in the case of the dBA. Figure 12 shows this difference clearly.

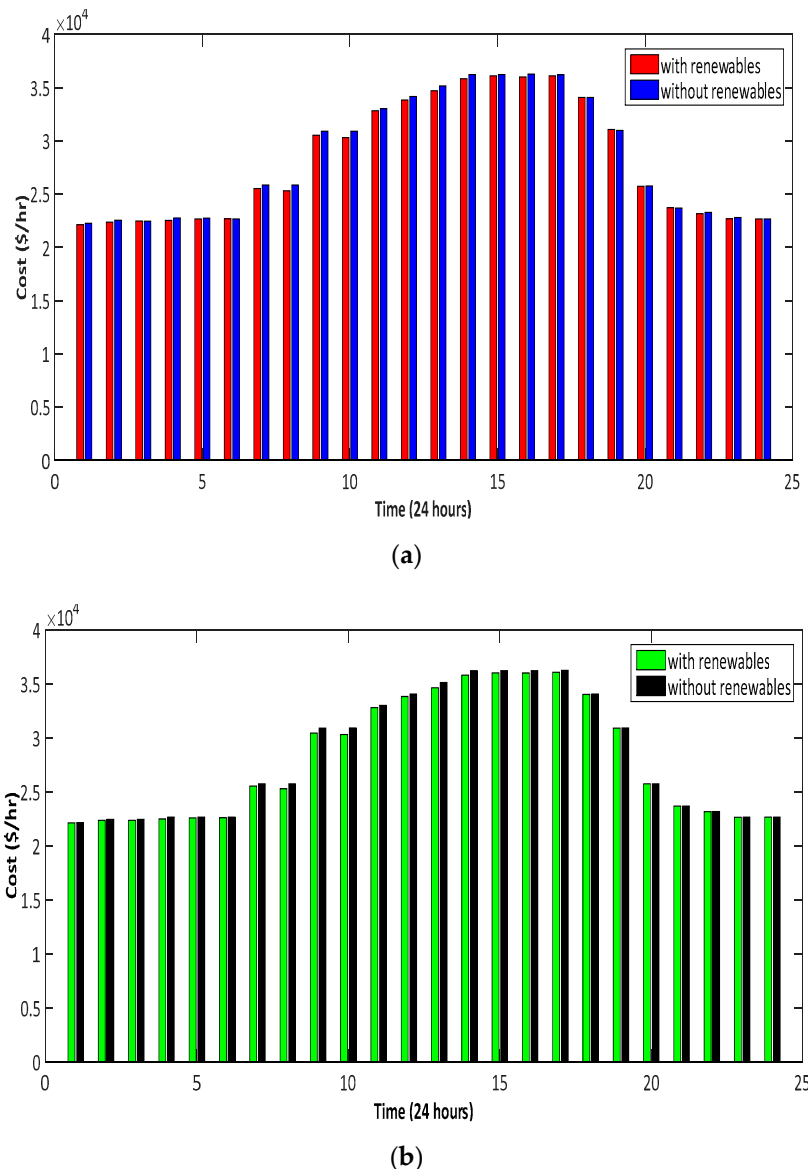


Figure 12. Cost offered by the (a) BA and (b) dBA without and with considering renewables.

4.2.3. Characteristics Offered by BA and dBA

Figures 13–17 show different convergence characteristics of the BA and dBA for selected test Case 2. The bat population was selected as 100, and total iterations were taken at 1000. Figures 13 and 14 show the position of bats of the BA and dBA, respectively at the start and after 1000 iterations. As observed from simulation results, bats start from a random location and converge to the best solution after 1000 iterations. It can also be seen that almost all the bats moved towards the best solution, showing that the solution is much closer to a global solution. However, in the case of the dBA, the bats are much better optimized. Figure 15a shows that the BA's fitness decreases very quickly, which increases the risk of capturing the local optimum solution. The fitness gradually decreases as the iteration increases. It gives a better chance of moving the solution closer to the global best position. Figure 15b shows the magnified view of the cost convergence curve. Figure 16 shows the pulse rate of the best bat, which

depicts the decrease of pulse rate as the bat finds its prey. Figure 17 shows the best bat's loudness, which depicts the increase of loudness as the bat finds its prey.

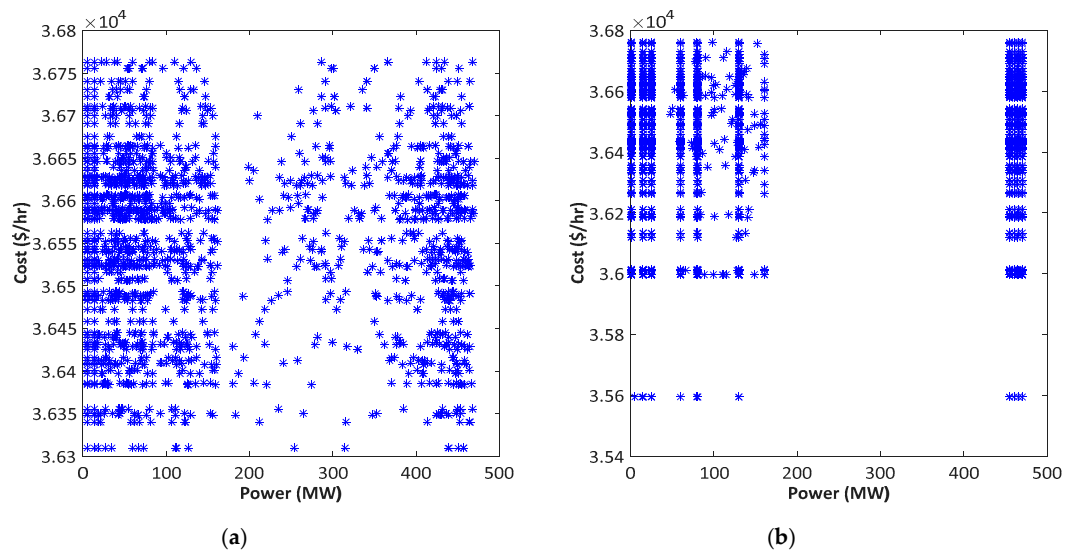


Figure 13. Bats positions in the BA (a) at the start and (b) after 1000 iterations (15-unit system with renewables).

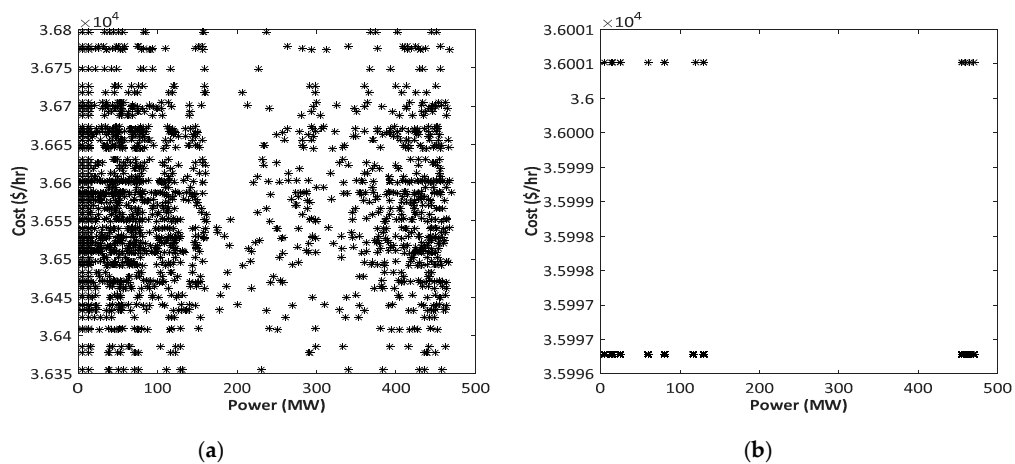


Figure 14. Bats positions in the dBA (a) before and (b) after 1000 iterations (15-unit system with renewables).

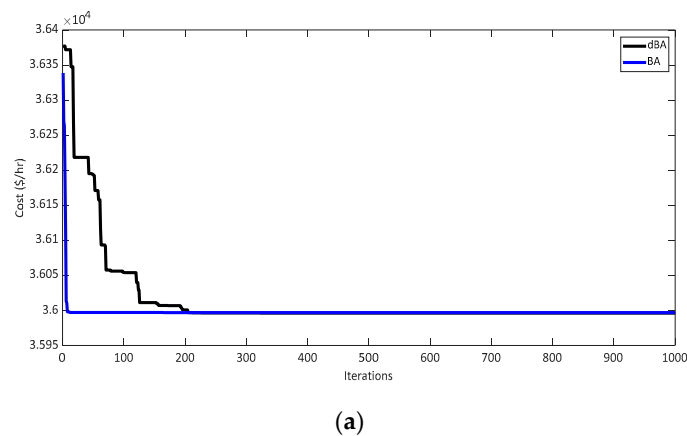


Figure 15. Cont.

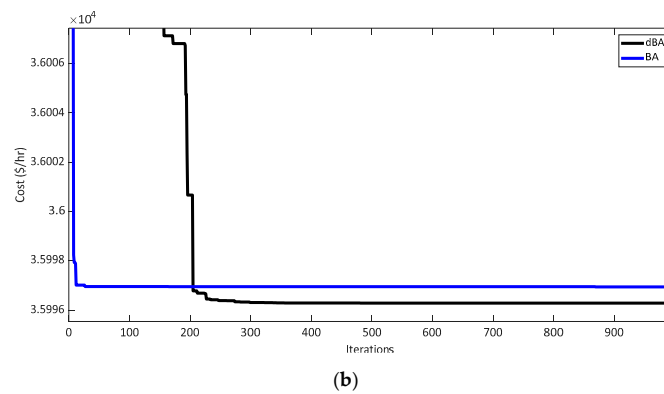


Figure 15. Convergence curve: (a) The cost convergence curve by the BA and dBA (15-unit system with renewables); (b) Magnified view.

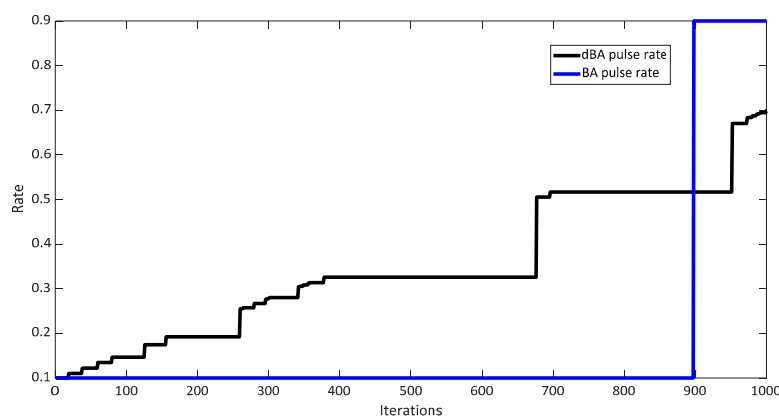


Figure 16. The pulse rate of the best bat of the BA and dBA.

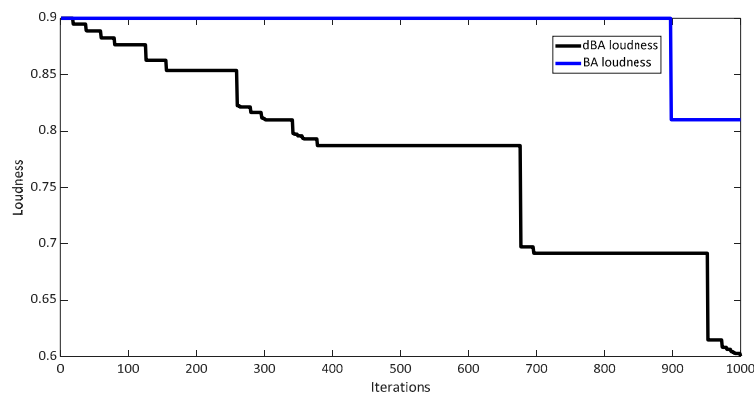


Figure 17. The loudness of the best bat of the BA and dBA.

4.2.4. Comparison of dBA, BA, PSO, and GA

Simulation results reveal that the variant dBA shows promising results in terms of better quality and convergence characteristics without being trapped in local optima compared to the conventional BA. To further validate the applicability of dBA, a test case of 3000 MW demand was taken and solved with population and iterations of 100 and 1000, respectively, using BA, dBA, PSO, and GA. Table 13 shows the result without renewables and Table 14 with renewables. It can be seen that the dBA tends to give better fitness than the BA, which in turn gives better results than that of the PSO and GA. Figures 18 and 19 depict the achievements regarding convergence characteristics.

Table 13. Cost comparison for 3000 MW demand without renewables.

Algo.	P_1 (MW)	P_2 (MW)	P_3 (MW)	P_4 (MW)	P_5 (MW)	P_6 (MW)	P_7 (MW)	P_8 (MW)	P_9 (MW)	P_{10} (MW)	P_{11} (MW)	P_{12} (MW)	P_{13} (MW)	P_{14} (MW)	P_{15} (MW)	Cost (\$/h)
GA	363.492	453.795	129.346	129.728	359.963	375.192	464.217	180.51	148.767	153.632	79.9023	77.2148	39.1577	27.5144	17.5699	3649
PSO	455	455	130	130	470	460	465	93.0009	162	25	20	80	25	15	15	36299
BA	454.98	454.98	129.98	129.98	469.98	459.98	464.98	60.01557	60.10281	159.98	20.01557	79.97995	25.01557	15.01557	15.01557	36242
dBA	455	455	130	130	470	460	465	60	25	135	80	80	25	15	15	36204

Table 14. Cost comparison for 3000 MW demand with renewables.

Algo.	P_1 (MW)	P_2 (MW)	P_3 (MW)	P_4 (MW)	P_5 (MW)	P_6 (MW)	P_7 (MW)	P_8 (MW)	P_9 (MW)	P_{10} (MW)	P_{11} (MW)	P_{12} (MW)	P_{13} (MW)	P_{14} (MW)	P_{15} (MW)	Wind (MW)	Solar (MW)	Cost (\$/h)
GA	359.14	361.427	129.932	129.952	388.694	362.319	390.447	290.997	150.702	153.982	78.889	78.993	55.887	34.555	15.079	13.71	5.3	36,491.1
PSO	455	455	130	130	470	460	465	60	25	75.9902	80	80	25	55	15	13.71	5.3	36,047
BA	454.91	454.909	129.909	129.909	469.909	459.909	464.909	60	25	116.809	79.909	79.909	25	15	15	13.71	5.3	35,996
dBA	455	455	130	130	470	460	465	60	25	115.99	80	80	25	15	15	13.71	5.3	35,995

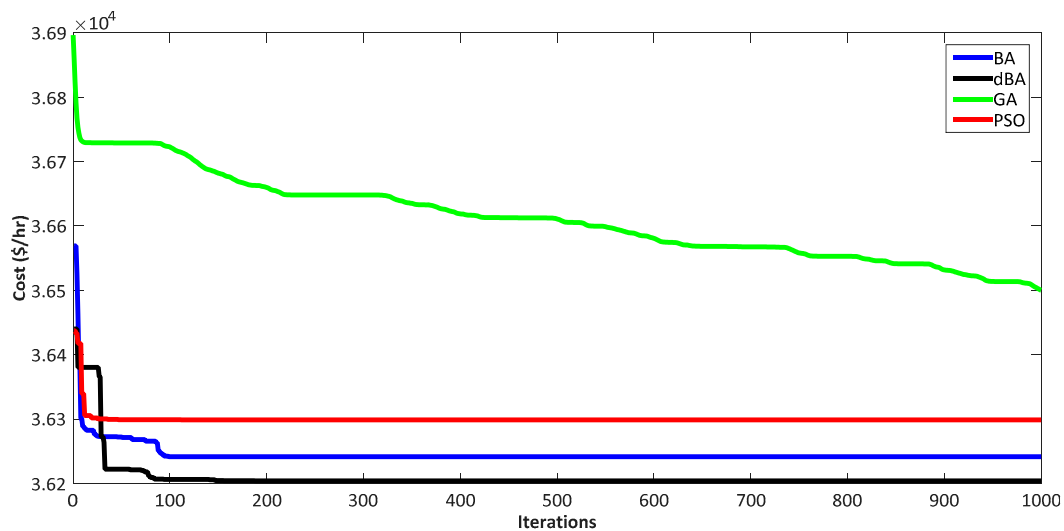


Figure 18. Convergence graphs for 3000 MW demand without renewables.

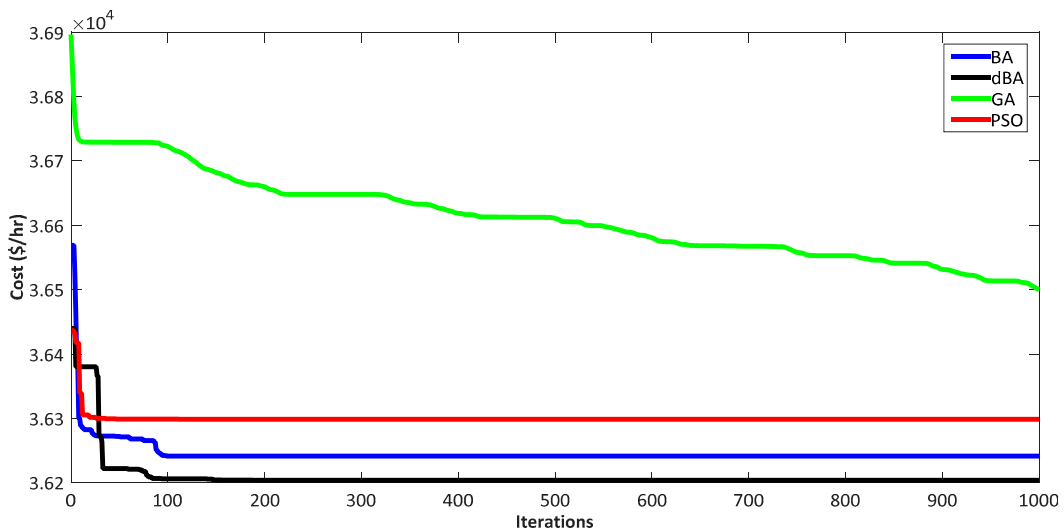


Figure 19. Convergence graphs for 3000 MW demand with renewables.

For all the scenarios considered in test cases, the dBA always performed better when compared to the BA and other metaheuristics such as the GA and PSO. This justifies the applicability and potency of dBA to renewables-incorporated ELD problems.

4.3. Case 3: 6 Thermal Units with Valve Point Effect

4.3.1. Data

An IEEE 30 bus system which consists of six thermal units running from fossil fuels with a valve point effect, is considered. The cost coefficients with minimum and maximum power generation limits are shown in Table 15 [26]. In Table 16, a 24 h load forecasting is selected as a load demand which is to be met. It can be seen that the maximum power demand at 1600 h is 1350 MW. In this case,

$$F_{thermal} = \sum_{i=1}^6 F_i(P_i).$$

Table 15. Cost coefficients of seven thermal units with lower and upper power limits.

Unit	a (\$/MW ²)	b (\$/MW)	c (\$)	e	f	P_{\min} (MW)	P_{\max} (MW)
1	0.007	7	240	300	0.031	100	500
2	0.0095	10	200	200	0.042	50	200
3	0.009	8.5	220	150	0.063	80	300
4	0.009	11	200	150	0.063	50	150
5	0.008	10.5	220	150	0.063	50	200
6	0.0075	12	190	150	0.063	50	120

Table 16. Demand forecasting over 24 h.

Time (h)	1	2	3	4	5	6	7	8	9	10	11	12
Demand (MW)	800	780	750	750	720	700	700	700	800	900	1000	1200
Time (h)	13	14	15	16	17	18	19	20	21	22	23	24
Demand (MW)	1260	1263	1300	1350	1100	900	850	800	780	750	700	800

The data used for RESs are mentioned where the renewables-incorporated ELD problem is discussed in the following sections/subsections.

4.3.2. Cost Offered by the BA and dBA

Table 17 shows the simulation results of the aBA and dBA in terms of operating cost for a 24 h period. It can be seen that the dBA comparatively gives less operating cost, i.e., 262,196.7 \$/day than that of the BA, which gives 263,734.7 \$/day. Even for most of the load demand for each hour, the dBA ensures a lower cost when compared to the BA. This ensures that the dBA displays a better global optimum solution with regards to the conventional BA. In the second scenario, a six-unit thermal system was added with one wind and one solar PV farm. Both BA and dBA were applied to ELD-incorporating renewables. Table 18 shows the result of the BA and dBA over a 24 h time period. It is clear from the results that the dBA gives better fitness results than the BA. The dBA is found to be more successful in reducing the total cost per day than the BA with or without renewables.

4.3.3. Comparison with Other Algorithms

To further justify the effectiveness of the dBA over the BA, PSO, GA, and enhanced bat algorithm (EBA) (another variant of BA), a test case of 1263 MW was taken. A population size of 50 and 200 iterations were taken for this case for all algorithms. The dBA was compared with the EBA, BA, PSO, and GA for an ELD problem without and with renewables. In [26], the EBA is already applied to the same 6-unit thermal system, taking the valve point effect. The parameters used for the EBA are the following: $f_{\min} = 0$, $f_{\max} = 2$, $r_0 = 0.5$, $A_0 = 0.9$, learning factor (ρ_{init}) = 0.65, and modulation Index (n) = 3. Table 19 shows a comparison of all mentioned techniques for the demand of 1263 MW. It can be seen that the dBA gives the lowest value when compared to other metaheuristic techniques. Table 20 shows a comparison of the same techniques without the EBA for a demand of 1263 MW. It can be seen that the dBA still gives the lowest value when compared to other metaheuristic techniques. Figure 20 shows the convergence graph without renewables, whereas Figure 21 shows the convergence with renewables, both for a load demand of 1263 MW.

Table 17. The BA and dBA on a six-thermal unit system without renewables.

<i>t</i> (h)	BA							dBA						
	<i>P</i> ₁ (MW)	<i>P</i> ₂ (MW)	<i>P</i> ₃ (MW)	<i>P</i> ₄ (MW)	<i>P</i> ₅ (MW)	<i>P</i> ₆ (MW)	Cost (\$/h)	<i>P</i> ₁ (MW)	<i>P</i> ₂ (MW)	<i>P</i> ₃ (MW)	<i>P</i> ₄ (MW)	<i>P</i> ₅ (MW)	<i>P</i> ₆ (MW)	Cost (\$/h)
1	304.0977	199.8699	145.6583	50.1247	50.1247	50.1247	9738.751	303.1211	50	197.1456	50	149.7333	50	9664.668
2	302.3879	50	277.6122	50	50	50	9360.333	400.2669	50	179.7331	50	50	50	9306.703
3	403.7476	50.0779	145.9411	50.0779	50.0779	50.0779	9065.843	302.6834	117.5835	80	99.8666	99.8666	50	9070.008
4	403.8278	116.1724	80	50	50	50	9074.849	404.0251	50	145.9749	50	50	50	9060.803
5	302.8308	50	80	50	187.1696	50	8837.094	302.6834	124.7998	142.5168	50	50	50	8663.793
6	404.1376	50	95.8625	50	50	50	8527.005	404.0251	65.9749	80	50	50	50	8540.125
7	403.6802	50	80	66.3199	50	50	8562.329	302.6834	50	197.3166	50	50	50	8451.905
8	304.9113	50	195.0889	50	50	50	8460.184	302.6834	50	179.7331	50	67.5835	50	8443.944
9	404.0628	50.0696	195.503	50.2274	50.0696	50.0696	9642.309	302.6834	117.717	179.7331	50	99.8666	50	9535.645
10	302.0052	198.8671	180.2607	50	50	118.8671	11,018.49	302.6834	124.7998	179.7331	50	192.7837	50	10,819.79
11	298.5139	119.4949	279.0726	50	155.4834	97.4355	12,188.55	302.6791	124.7997	272.9238	99.8665	99.8665	99.8643	12,066.25
12	405.8937	196.2599	279.4071	116.9151	150.0368	51.4876	14,667.56	404.0251	200	229.5997	116.7756	149.7331	99.8666	14,613.49
13	405.654	198.2898	257.4718	149.9055	198.6867	50	15,458.83	404.0251	199.5997	229.5997	149.7331	177.176	99.8666	15,423
14	499.7773	199.4551	264.276	50	199.4917	50	15,545.15	404.0251	180.176	229.5997	149.7331	199.5997	99.8666	15,459.25
15	499.9861	121.895	229.7232	149.6276	199.9861	98.782	15,923.5	496.4093	124.7986	279.4612	149.7312	149.7331	99.8665	15,899.96
16	499.7221	199.5299	251.3507	149.8015	199.596	50	16,678.19	500	199.5997	251.0676	99.8666	199.5997	99.8666	16,668
17	410.8341	199.6708	229.0246	50.0123	111.3209	99.1373	13,400.56	404.0303	199.5999	246.6364	99.8667	50	99.8667	13,397.62
18	302.8311	125.9796	222.1654	149.0241	50	50	10,863.54	302.6834	117.9839	229.5997	50	149.7331	50	10,767.51
19	495.3723	124.6277	80	50	50	50	10,415.96	404.0251	116.2418	179.7331	50	50	50	10,156.68
20	404.015	50.1457	195.4023	50.1457	50.1457	50.1457	9642.712	302.6834	124.7998	179.7331	50	50	92.7837	9604.737
21	302.2643	50	129.2625	50	198.4738	50	9408.851	400.2669	50	179.7331	50	50	50	9306.703
22	404.6521	50	145.348	50	50	50	9064.374	302.6834	67.717	229.5997	50	50	50	9048.594
23	404.2485	50	80	50	65.7516	50	8548.91	302.6834	67.5835	80	149.7331	50	50	8634.162
24	403.986	50	196.0141	50	50	50	9640.874	403.9045	116.2324	129.8639	50	50	50	9593.417
	Total Cost (\$/day)						263,734.7	Total Cost (\$/day)						262,196.7

Table 18. The BA and dBA on a six-thermal unit system with renewables (wind and solar).

<i>t</i> (h)	BA									dBA									
	<i>P</i> ₁ (MW)	<i>P</i> ₂ (MW)	<i>P</i> ₃ (MW)	<i>P</i> ₄ (MW)	<i>P</i> ₅ (MW)	<i>P</i> ₆ (MW)	Wind (MW)	Solar (MW)	Cost	<i>P</i> ₁ (MW)	<i>P</i> ₂ (MW)	<i>P</i> ₃ (MW)	<i>P</i> ₄ (MW)	<i>P</i> ₅ (MW)	<i>P</i> ₆ (MW)	Wind (MW)	Solar (MW)	Cost (\$/h)	
1	407.261	50	191.0391	50	50	50	1.7	0	9623.146	302.6924	50	229.6642	50	115.9815	50	302.6924	0	9626.532	
2	403.9725	50	80	137.5276	50	50	8.5	0	9454.004	216.713	124.8317	179.7337	50.3936	149.8281	50.0001	216.713	0	9422.702	
3	407.4166	52.8849	80	100.4289	50	50	9.27	0	8997.98	302.1017	109.632	179.253	50	50	50	302.1017	0	8912.984	
4	302.8392	50	229.3799	51.1211	50	50	16.7	0	8743.5	302.8251	50	130.7264	99.9077	99.8885	50	302.8251	0	8767.597	
5	301.2707	50	211.5096	50	50	50	7.22	0	8625.025	302.6834	50	80	80.3635	149.7331	50	302.6834	0	8746.108	
6	309.4563	50	185.6037	50	50	50	4.91	0.03	8371.869	302.6977	61.0559	179.8242	50.0208	50.0004	51.4948	302.6977	0.03	8357.135	
7	399.07	50	80	50	50	50	14.7	6.27	8222.705	302.6795	50	176.3905	50	50	50	302.6795	6.27	8101.709	
8	303.8568	122.6032	80	50	50	50	26.6	17	7916.233	226.7368	50	129.9616	99.8799	99.8826	50	226.7368	17	8147.866	
9	300.4229	127.362	177.1759	50.0366	50.0366	50.0366	20.9	24.1	9027.041	302.6734	50.1159	129.9708	99.9166	99.5375	72.8991	302.6734	24.1	9195.099	
10	404.5675	50	232.997	55.2156	50	50	17.9	39.4	10,125.3	404.0079	58.2945	179.8913	99.9727	50.5936	50.0207	404.0079	39.4	10,114.19	
11	405.3966	130.018	185.9864	103.5525	50.1832	104.6533	12.8	7.41	11,927.35	404.0191	50	179.7296	146.318	149.7246	50	404.0191	7.41	11,788.42	
12	402.9712	199.5415	276.0535	96.2798	152.7847	50.0694	18.7	3.65	14,292.73	404.4885	124.7998	279.4668	119.2786	149.8399	99.8314	404.4885	3.65	14,334.4	
13	499.4858	189.1041	227.7647	147.7838	99.5717	50	14.4	31.9	14,891.31	404.1383	130.5086	229.6849	149.6973	199.6692	100.0118	404.1383	31.9	14,727.89	
14	403.9604	196.115	278.8123	50	199.2537	97.6997	10.4	26.8	14,922.88	404.0251	193.019	229.563	149.7223	199.536	50	404.0251	26.8	14,888.17	
15	499.9823	50.364	279.7122	149.9823	199.9823	101.637	8.26	10.1	15,777.14	500	124.7999	279.4662	149.732	149.7337	77.9305	500	10.1	15,773.39	
16	499.9947	199.48	280.3615	100.7151	199.9947	50.446	13.7	5.3	16,302.84	500	199.8978	279.5025	149.999	150.4317	51.1593	500	5.3	16,297.56	
17	404.8324	199.9615	280.2751	50.2983	50.2983	101.3246	3.44	9.57	13,175.66	404.0315	124.5384	229.5879	99.859	129.2	99.7795	404.0315	9.57	13,158.34	
18	301.0121	198.385	178.1683	50	50	118.2546	1.87	2.31	10,989.48	308.9345	57.3585	229.7199	50.0997	149.8421	99.8655	308.9345	2.31	10,855.5	
19	303.5578	50	195.8985	50	199.7937	50	0.75	0	10,321.21	302.6831	121.8288	129.8605	98.6726	99.8539	96.3515	302.6831	0	10,242.29	
20	303.4517	50.0205	279.1827	50	67.1753	50	0.17	0	9713.297	204.3773	50.1842	279.4667	66.0672	99.8678	99.8667	204.3773	0	9922.678	
21	302.3867	50.3536	176.8755	149.5274	50.3536	50.3536	0.15	0	9399.814	302.6804	50	179.7224	97.5928	99.854	50.0005	302.6804	0	9300.974	
22	405.7363	50.8019	80.8019	51.3261	109.8055	51.2187	0.31	0	9155.692	302.6833	117.311	80.0002	99.8299	99.8656	50	302.6833	0	9069.648	
23	404.8733	64.0576	80	50	50	50	1.07	0	8525.123	302.6835	50.0002	146.3776	99.8665	50	50.0022	302.6835	0	8473.289	
24	302.5694	50	232.2333	50	50	114.6174	0.58	0	9750.315	403.9456	115.6947	80	99.8031	50	50	403.9456	0	9689.647	
	Total Cost (\$/day)									Total Cost (\$/day)									257,914.1

Table 19. Comparison of the dBA, enhanced bat algorithm (EBA), BA, PSO, and GA without renewables.

Unit	dBA	EBA [26]	BA	PSO	GA
1	404.0243	404.0251	403.8001	500	402.7638
2	199.5995	199.5997	199.7978	200	186.9464
3	260.0438	279.4662	224.1185	229.4894	279.9828
4	149.7328	149.7331	148.2026	150	99.8815
5	149.7333	180.1760	198.3771	133.5109	188.7443
6	99.8664	50	88.70405	50	104.681
P_{GTOTAL} (MW)	1263	1263	1263	1263	1263
Cost (\$/h)	15,448.9331	15,453.8841	15,498.9328	15,524.9449	15,563.0527

Table 20. Comparison of the dBA, BA, PSO, and GA with renewables.

Unit	dBA	BA	PSO	GA
1	404.0152	402.1131	500	499.9096
2	124.3873	125.9102	126.6186	147.8697
3	229.5998	280.6446	229.5035	229.9327
4	149.2019	149.4743	50	101.3156
5	198.8925	197.6381	200	149.7285
6	99.6837	50	99.6575	77.02417
Wind	17.85	17.85	17.85	17.85
Solar PV	39.37	39.37	39.37	39.37
P_{GTOTAL} (MW)	1263	1263	1263	1263
Cost (\$/h)	14,592.6446	14,632.51	14,698.722	14,944.389

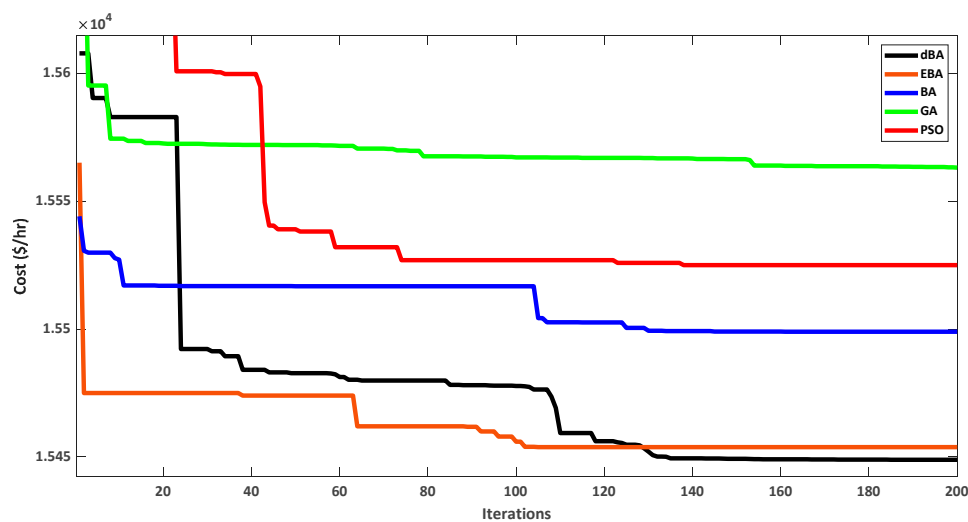


Figure 20. Cost convergence graph with valve point effect without renewables.

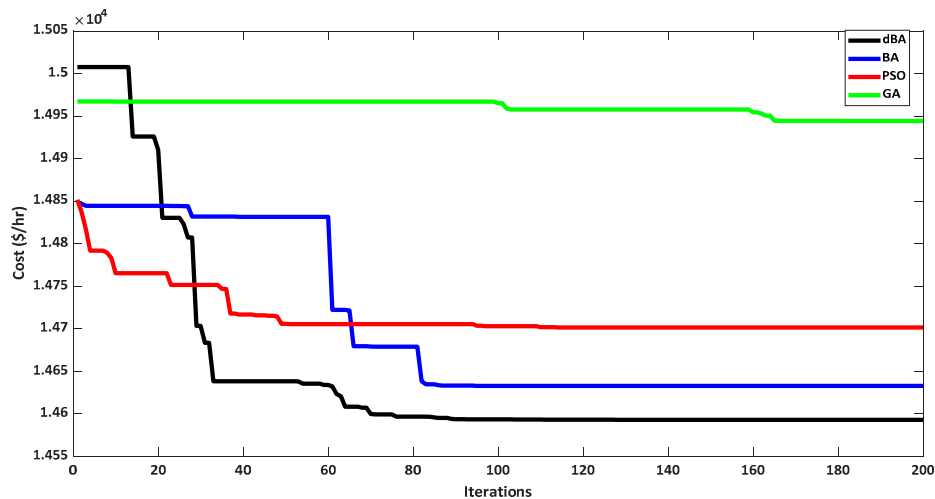


Figure 21. Cost convergence graph with the valve point effect and renewables.

4.4. Case 4

To further compare the effectiveness of the dBA with other metaheuristic techniques, in this case study, a 150 kV power system located in East Java, Indonesia, consisting of 10 units, is considered. Cost coefficients of the units with lower and upper power bounds, taken from [51], are summarized in Table 21. The total system demand without the transmission losses is 616 MW. Population size and iterations are kept the same for all the techniques to compare the results on one scale.

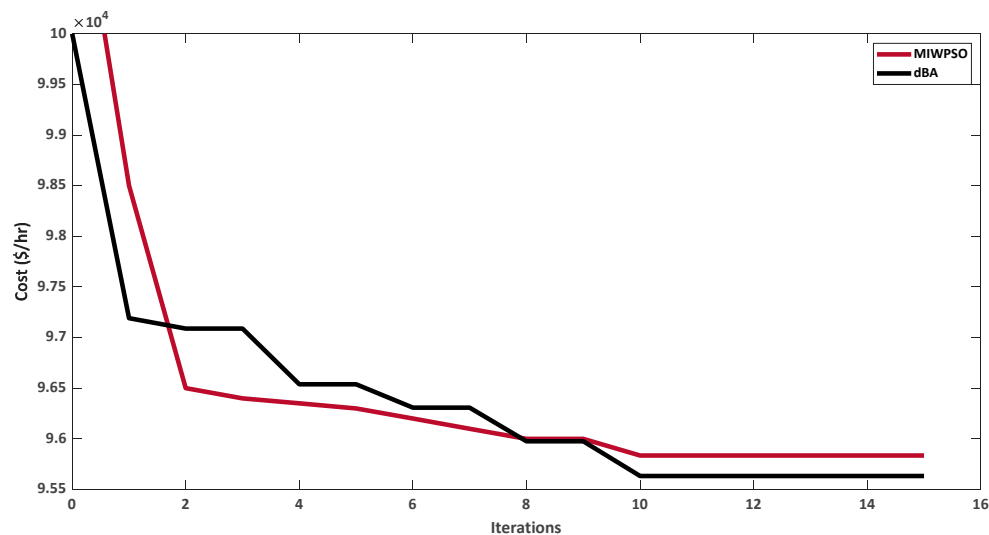
Table 21. A 10-unit thermal system cost coefficients with lower and upper power limits.

Generator	a (\$/MW ²)	b (\$/MW)	c (\$)	P_{\min} (MW)	P_{\max} (MW)
1	0.2162	42.5118	4088.5375	23	92
2	0.4108	20.5021	4547.8075	23	92
3	0.0562	32.9483	4601.9649	47.25	189
4	0.1266	22.2655	4316.1074	47.25	189
5	0.6210	50.6244	3707.7500	10.25	41
6	0.1255	69.7050	3459.6950	10.25	41
7	3.6454	370.6642	9045.7750	23	95
8	0.3981	31.9013	1124.9075	23	95
9	2.3185	484.7006	8549.5500	23	95
10	0.1142	31.8112	4486.6174	41.25	165

A comparison of the results offered by the dBA and other algorithms such as the BA, GA, PSO, and modified inertial weight-based PSO (MIW-PSO) is presented in Table 22. The dBA offers a low cost, i.e., 95,633 \$/h when compared to all other mentioned techniques, thus validating the workability of the dBA. This low cost is also depicted in the convergence characteristics drawn for the dBA and MIWPSO, as shown in Figure 22. For the comparison purpose, the convergence characteristics are drawn for 15 iterations.

Table 22. Comparison of dBA, BA, GA, PSO, and modified inertial weight-based PSO (MIW-SPO).

Generator	dBA	BA	GA	PSO [51]	MIW-PSO [51]
1	35.84	23	42.469	38.63	36.34
2	44.47	52.51	54.964	38.94	46.58
3	189	185.97	69.765	178	189
4	138.40	150.56	73.755	142.20	139.16
5	10.25	10.25	32.788	13.43	11.06
6	10.25	10.25	37.772	13.42	10.25
7	23	23	23.009	29	23
8	31.62	23	93.591	26.84	29.90
9	23	23	23.032	29	23
10	110.17	114.47	164.854	106.54	107.71
P_{GTOTAL} (MW)	616	616	616	616	616
Cost (\$/h)	95,633.00	95,745.54	100,207.15	95,840.57	95,835.53

**Figure 22.** Cost convergence graph of the dBA and MIWPSO in a 10-unit system case.

From the inspection of the convergence characteristics of all the considered case studies, we observed that at the initial stage, the dBA almost converges slowly compared to other algorithms due to a rigorous exploration process to ensure effective search space exploration. However, as the algorithm progresses, the exploitation dominates exploration to speed up the convergence toward global optimum compared to other algorithms. The dBA boosts its exploration and exploitation capabilities due to the introduction of directional echolocation to the structure of BA, the inclusion of a scale factor in the local search step to make the movement random, thus avoiding a local convergence, the acceptance of new solutions based on a random value to ameliorate the solution quality, and monotonically increasing and decreasing pulse rate and loudness, respectively, to enhance diversity. In this way, the dBA offers promising convergence characteristics compared to other algorithms, giving a low total fuel cost. We also noticed that the algorithm performs better as the problems' dimensions increase because of its capability to promote diversity and avoid the local optima.

5. Conclusions

In this paper, the modified directional bat algorithm (dBA), which is a useful variant of nature-inspired (BA), was utilized to solve the ELD problem with and without the optimal integration of RESs such as solar and wind. The dominance of this metaheuristic technique was highlighted by comparing the performance of the dBA with BA and other prominent metaheuristics techniques like GA and PSO. Moreover, to show the superiority of the dBA, it was also compared with the variants of PSO and BA such as MIWPSO and EBA. Different test cases were considered to analyze and compare the performance of the dBA. From the simulation results, it could be seen that by incorporating renewables in the thermal unit system, the operating cost of the system decreased significantly. Moreover, with the help of directional echolocation, the dBA outperformed all other algorithms with comparatively fast convergence. It also reduced the probability of a premature convergence problem due to the elitism mechanism. In addition, the valve point effect was also considered to test the algorithm with a more practical system. In future, this improved variant of the BA could be applied to even more realistic ELD problems taking more practical constraints such as prohibited operating zones, multiple fuel options, and transmission losses along with other renewables.

Author Contributions: Conceptualization, F.T. and G.A.; Data curation, S.A.; Formal analysis, G.A. and M.R.H.; Funding acquisition, S.A.; Investigation, G.A.; Methodology, F.T.; Project administration, G.A.; Resources, M.R.H.; Software, A.Q.; Visualization, S.A.; Writing—original draft, F.T.; Writing—review & editing, A.Q. All authors have read and agreed to the published version of the manuscript.

Funding: This research is financially supported by the Deanship of Scientific Research at King Khalid University under research grant number (R.G.P2/100/41).

Acknowledgments: The authors extend their appreciation to the Deanship of Scientific Research, King Khalid University under research grant number (R.G.P2/100/41). The authors would like to express their gratitude to The University of Lahore for the administrative and technical support.

Conflicts of Interest: The authors declare no conflict of interest.

References

1. Niknam, T.; Azizipanah-Abarghooee, R.; Aghaei, J. A new modified teaching-learning algorithm for reserve constrained dynamic economic dispatch. *IEEE Trans. Power Syst.* **2012**, *28*, 749–763. [[CrossRef](#)]
2. Park, J.-B.; Lee, K.-S.; Shin, J.-R. A particle swarm optimization for economic dispatch with nonsmooth cost functions. *IEEE Trans. Power Syst.* **2005**, *20*, 34–42. [[CrossRef](#)]
3. Puri, V.; Chauhan, Y.K. A solution to economic dispatch problem using augmented Lagrangian particle swarm optimization. *Int. J. Emerg. Technol. Adv. Eng. ISSN* **2012**, 2250–2459.
4. Park, J.-B.; Jeong, Y.-W.; Shin, J.-R.; Lee, K.Y. An improved particle swarm optimization for nonconvex economic dispatch problems. *IEEE Trans. Power Syst.* **2009**, *25*, 156–166. [[CrossRef](#)]
5. Yang, Y.; Wei, B.; Liu, H.; Zhang, Y.; Zhao, J.; Manla, E. Chaos firefly algorithm with self-adaptation mutation mechanism for solving large-scale economic dispatch with valve-point effects and multiple fuel options. *IEEE Access* **2018**, *6*, 45907–45922. [[CrossRef](#)]
6. Vo, D.N.; Schegner, P.; Ongsakul, W. Cuckoo search algorithm for non-convex economic dispatch. *IET Gener. Transm. Distrib.* **2013**, *7*, 645–654. [[CrossRef](#)]
7. Niknam, T.; Golestaneh, F. Enhanced bee swarm optimization algorithm for dynamic economic dispatch. *IEEE Syst. J.* **2013**, *7*, 754–762. [[CrossRef](#)]
8. Zaman, M.F.; Elsayed, S.M.; Ray, T.; Sarker, R.A. Evolutionary algorithms for dynamic economic dispatch problems. *IEEE Trans. Power Syst.* **2016**, *31*, 1486–1495. [[CrossRef](#)]
9. Dekhici, L.; Borne, P.; Khaled, B. Firefly algorithm for economic power dispatching with pollutants emission. *Inform. Econ.* **2012**, *16*, 45–57.
10. Zhao, J.; Liu, S.; Zhou, M.; Guo, X.; Qi, L. Modified cuckoo search algorithm to solve economic power dispatch optimization problems. *IEEE/CAA J. Autom. Sin.* **2018**, *5*, 794–806. [[CrossRef](#)]
11. Ma, X.; Liu, Y. Particle swarm optimization to solving economic load dispatch with spinning reserve. In Proceedings of the 2010 International Conference on Computer Design and Applications, Qinhuangdao, China, 25–27 June 2010; Volume 4, pp. V4–214–V4–217.

12. Gaing, Z.-L. Particle swarm optimization to solving the economic dispatch considering the generator constraints. *IEEE Trans. Power Syst.* **2003**, *18*, 1187–1195. [[CrossRef](#)]
13. Meng, K.; Wang, H.-G.; Dong, Z.; Wong, K.P. Quantum-inspired particle swarm optimization for valve-point economic load dispatch. *IEEE Trans. Power Syst.* **2009**, *25*, 215–222. [[CrossRef](#)]
14. Abdullah, N.R.H.; Ghazali, N.; Ibrahim, N.; Solleh, N.F.; Samad, R.; Mustafa, M.; Pebrianti, D. Solving economic dispatch (ED) problem using artificial immune system, evolutionary programming and particle swarm optimization. *ARPN J. Eng. Appl. Sci.* **2006**, *11*, 6663–6667.
15. Khamsawang, S.; Jiriwibhakorn, S. Solving the economic dispatch problem using novel particle swarm optimization. *World Acad. Sci. Eng. Technol.-Int. J. Electr. Comput. Energ. Electron. Commun. Eng.* **2009**, *3*, 529–534.
16. Abbas, G.; Gu, J.; Farooq, U.; Asad, M.U.; El-Hawary, M. Solution of an economic dispatch problem through particle swarm optimization: A detailed survey-Part I. *IEEE Access* **2017**, *5*, 15105–15141. [[CrossRef](#)]
17. Abbas, G.; Gu, J.; Farooq, U.; Raza, A.; Asad, M.U.; El-Hawary, M.E. Solution of an economic dispatch problem through particle swarm optimization: A detailed survey; Part II. *IEEE Access* **2017**, *5*, 24426–24445. [[CrossRef](#)]
18. Trivedi, I.N.; Jangir, P.; Bhoje, M.; Jangir, N. An economic load dispatch and multiple environmental dispatch problem solution with microgrids using interior search algorithm. *Neural Comput. Appl.* **2018**, *30*, 2173–2189. [[CrossRef](#)]
19. Biswal, S.; Barisal, A.K.; Behera, A.; Prakash, T. Optimal power dispatch using BAT algorithm. In Proceedings of the 2013 International Conference on Energy Efficient Technologies for Sustainability, Nagercoil, India, 10–12 April 2013; pp. 1018–1023.
20. Sakthivel, S.; Natarajan, R.; Gurusamy, P. Application of bat optimization algorithm for economic load dispatch considering valve point effects. *Int. J. Comput. Appl.* **2013**, *67*, 35–39. [[CrossRef](#)]
21. Nguyen, T.T.; Ho, S.D. Bat algorithm for economic emission load dispatch problem. *Int. J. Adv. Sci. Technol.* **2016**, *86*, 51–60. [[CrossRef](#)]
22. Gherbi, Y.A.; Bouzeboudja, H.; Lakdja, F. Economic dispatch problem using bat algorithm. *Leonardo J. Sci.* **2014**, *24*, 75–84.
23. Latif, A.; Palensky, P. Economic dispatch using modified bat algorithm. *Algorithms* **2014**, *7*, 328–338. [[CrossRef](#)]
24. Niknam, T.; Azizipanah-Abarghooee, R.; Zare, M.; Bahmanifirouzi, B. Reserve constrained dynamic environmental/economic dispatch: A new multiobjective self-adaptive learning bat algorithm. *IEEE Syst. J.* **2013**, *7*, 763–776. [[CrossRef](#)]
25. Adarsh, B.; Raghunathan, T.; Jayabarathi, T.; Yang, X.-S. Economic dispatch using chaotic bat algorithm. *Energy* **2016**, *96*, 666–675. [[CrossRef](#)]
26. Pradhan, G.; Dewangan, P.D. Solving optimal load dispatch problem using enhanced BAT optimization algorithm. In Proceedings of the 2017 Innovations in Power and Advanced Computing Technologies (i-PACT), Vellore, India, 21–22 April 2017; pp. 1–6.
27. Fister, I.; Yang, X.-S.; Fong, S.; Zhuang, Y. Bat algorithm: Recent advances. In Proceedings of the 2014 IEEE 15th International Symposium on Computational Intelligence and Informatics (CINTI), Budapest, Hungary, 19–21 November 2014; pp. 163–167.
28. Gautham, S.; Rajamohan, J. Economic load dispatch using novel bat algorithm. In Proceedings of the 2016 IEEE 1st International Conference on Power Electronics, Intelligent Control and Energy Systems (ICPEICES), Dehli, India, 4–6 July 2016; pp. 1–4.
29. Liang, H.; Liu, Y.; Shen, Y.; Li, F.; Man, Y. A hybrid bat algorithm for economic dispatch with random wind power. *IEEE Trans. Power Syst.* **2018**, *33*, 5052–5061. [[CrossRef](#)]
30. Osório, G.; Lujano-Rojas, J.; Matias, J.C.D.O.; Catalão, J.P. A probabilistic approach to solve the economic dispatch problem with intermittent renewable energy sources. *Energy* **2015**, *82*, 949–959. [[CrossRef](#)]
31. Nikmehr, N.; Ravadanegh, S.N. A study on optimal power sharing in interconnected microgrids under uncertainty. *Int. Trans. Electr. Energy Syst.* **2015**, *26*, 208–232. [[CrossRef](#)]
32. Khan, N.A.; Awan, A.B.; Mahmood, A.; Razzaq, S.; Zafar, A.; Sidhu, G.A.S. Combined emission economic dispatch of power system including solar photo voltaic generation. *Energy Convers. Manag.* **2015**, *92*, 82–91. [[CrossRef](#)]
33. Farhat, I.; El-Hawary, M. Dynamic adaptive bacterial foraging algorithm for optimum economic dispatch with valve-point effects and wind power. *IET Gener. Transm. Distrib.* **2010**, *4*, 989. [[CrossRef](#)]

34. Li, Z.; Wu, W.; Zhang, B.; Sun, H.; Yang, Y. Dynamic economic dispatch using Lagrangian relaxation with multiplier updates based on a quasi-newton method. *IEEE Trans. Power Syst.* **2013**, *28*, 4516–4527. [[CrossRef](#)]
35. Han, L.; Romero, C.E.; Wang, X.; Shi, L. Economic dispatch considering the wind power forecast error. *IET Gener. Transm. Distrib.* **2018**, *12*, 2861–2870. [[CrossRef](#)]
36. Brini, S.; Abdallah, H.H.; Ouali, A. Economic dispatch for power system included wind and solar thermal energy. *Leonardo J. Sci.* **2009**, *14*, 204–220.
37. Warsono; King, D.J.; Ozveren, C.S.; Bradley, D. Economic load dispatch optimization of renewable energy in power system using genetic algorithm. In Proceedings of the 2007 IEEE Lausanne Power Tech, Lausanne, Switzerland, 1–5 July 2007; pp. 2174–2179.
38. Roy, S. Inclusion of short duration wind variations in economic load dispatch. *IEEE Trans. Sustain. Energy* **2012**, *3*, 265–273. [[CrossRef](#)]
39. Jadoun, V.K.; Pandey, V.C.; Gupta, N.; Niazi, K.R.; Swarnkar, A. Integration of renewable energy sources in dynamic economic load dispatch problem using an improved fireworks algorithm. *IET Renew. Power Gener.* **2018**, *12*, 1004–1011. [[CrossRef](#)]
40. Tang, C.; Xu, J.; Tan, Y.; Sun, Y.; Zhang, B. Lagrangian relaxation with incremental proximal method for economic dispatch with large numbers of wind power scenarios. *IEEE Trans. Power Syst.* **2019**, *34*, 2685–2695. [[CrossRef](#)]
41. Kheshti, M.; Kang, X.; Li, J.; Regulski, P.; Terzija, V. Lightning flash algorithm for solving non-convex combined emission economic dispatch with generator constraints. *IET Gener. Transm. Distrib.* **2018**, *12*, 104–116. [[CrossRef](#)]
42. Nivedha, R.R.; Singh, J.G.; Ongsakul, W. PSO based economic dispatch of a hybrid microgrid system. In Proceedings of the 2018 International Conference on Power, Signals, Control and Computation (EPSCICON), Thrissur, India, 6–10 January 2018; pp. 1–5.
43. Augustine, N.; Suresh, S.; Moghe, P.; Sheikh, K. Economic dispatch for a microgrid considering renewable energy cost functions. In Proceedings of the 2012 IEEE PES Innovative Smart Grid Technologies (ISGT), Washington, DC, USA, 16–20 January 2020; pp. 1–7.
44. Agrawal, S.P.; Porate, K.B. Economic dispatch of thermal units with the impact of wind power plant. In Proceedings of the 2010 3rd International Conference on Emerging Trends in Engineering and Technology, Goa, India, 19–21 November 2020; pp. 48–53.
45. Jose, J.T. Economic load dispatch including wind power using Bat Algorithm. In Proceedings of the 2014 International Conference on Advances in Electrical Engineering (ICAEE), Singapore, Singapore, 19 February 2014; pp. 1–4.
46. Ellahi, M.; Abbas, G.; Khan, I.; Koola, P.M.; Nasir, M.; Raza, A.; Farooq, U. Recent approaches of forecasting and optimal economic dispatch to overcome intermittency of wind and Photovoltaic (PV) systems: A review. *Energies* **2019**, *12*, 4392. [[CrossRef](#)]
47. Yang, X.-S. A new metaheuristic bat-inspired algorithm. In *Nature Inspired Cooperative Strategies for Optimization (NICSO 2010)*; Springer: Berlin/Heidelberg, Germany, 2010; pp. 65–74.
48. Chakri, A.; Khelif, R.; Benouaret, M.; Yang, X.-S. New directional bat algorithm for continuous optimization problems. *Expert Syst. Appl.* **2017**, *69*, 159–175. [[CrossRef](#)]
49. Chakri, A.; Ragueb, H.; Yang, X.-S. Bat algorithm and directional bat algorithm with case studies. In *Nature-Inspired Algorithms and Applied Optimization*; Springer: Cham, Switzerland, 2018; pp. 189–216.
50. Rahmat, N.A.; Aziz, N.F.A.; Mansor, M.H.; Musirin, I. Optimizing economic load dispatch with renewable energy sources via differential evolution immunized ant colony optimization technique. *Int. J. Adv. Sci. Eng. Inf. Technol.* **2017**, *7*, 2012–2017. [[CrossRef](#)]
51. Lee, C.-Y.; Tuegeh, M. An optimal solution for smooth and non-smooth cost functions-based economic dispatch problem. *Energies* **2020**, *13*, 3721. [[CrossRef](#)]

Publisher’s Note: MDPI stays neutral with regard to jurisdictional claims in published maps and institutional affiliations.



© 2020 by the authors. Licensee MDPI, Basel, Switzerland. This article is an open access article distributed under the terms and conditions of the Creative Commons Attribution (CC BY) license (<http://creativecommons.org/licenses/by/4.0/>).